Masterarbeit am Institut für Mathematik der Freien Universität Berlin

Computing the minimal rebinding effect for nonreversible processes

Susanne Röhl

Matrikelnummer: 4364172

susanne.roehl@fu-berlin.de

Betreuer: PD Dr. Marcus Weber

Zweitgutachter: PD Dr. Konstantin Fackeldey

Berlin, 4. September 2017

Abstract

The aim of this thesis is to investigate the rebinding effect, a phenomenon describing a "short-time memory" which can occur when projecting a Markov process onto a finite state space. Under the assumption of a fuzzy clustering in terms of membership functions, a minimal bound for the rebinding effect included in a given system is computed as the solution of an optimization problem. Based on membership functions $\chi = XA$, being a linear combination of Schur vectors, this generalized approach includes reversible as well as non-reversible processes.

Contents

Introduction

Markov processes are memoryless stochastic processes with applications in many different kinds of areas. They are employed to describe molecular systems like protein folding[11] or ligand-binding processes[43]. Such processes act on very large state spaces and additionally require simulations on rather long time-scales in order to observe rare conformational changes. Consequently, a reduction of dimension is aimed at, which can be realized by a projection onto a smaller state space. The reduced model should represent the correct long-time behaviour of the process, while being less complex. The existence of metastable sets can be exploited to create such a "Markov State Model"[5, 10]. A well-established solution is the fuzzy clustering algorithm PCCA+, which identifies metastable sets with the aid of membership functions $\chi = XA$, being a linear combination of eigenvectors[52].

When projecting a process onto a finite state space, it can lose its Markov property, more precisely it can include short-time memory effects. Such memory effects were detected in the context of ligand-binding-systems, where in certain configurations significantly increased binding affinities were observed[50]. They are explained by an additional memory caused by the projection: short time after a ligand unbound from its target, it is assumed to be still nearby and thus rebinds with a high probability. Consequently, this short-time memory is denoted as **rebinding effect**. This memory effect is strongly related to the **overlap** of the membership functions χ determining the clustering. Hence, knowing them makes it easy to compute the actual rebinding effect caused by this projection. However, in many cases the original process and the membership functions are not known. For instance, a finite process can be constructed as the solution of a differential equation and just be interpreted as the projection of a larger process. In order to identify possible memory effects included in that system, it is favorable to estimate the rebinding effect. This can be achieved by solving an optimization problem, revealing a minimal bound:

"Given a clustered system, how much rebinding is included **at least**?"

The computation of the minimal rebinding effect included in a given kinetics has been accomplished for reversible processes in 2014 by Weber and Fackeldey[56]. In this thesis, the formulation of the corresponding optimization problem is extended onto non-reversible processes. This is achieved by employing the framework of GenPCCA, a recent modification of PCCA+ by Weber and Fackeldey[54] from 2017, which is based on Schur vectors instead of eigenvectors and includes non-reversible processes. This generalization is of particular interest since many real-world processes are non-reversible[17].

A significant application of the presented topic lies in the area of computational drug design. In order to treat diseases, ligands are designed such that they bind to pathogenic target molecules. Improving the binding affinity is one important goal in drug design. For a precise prediction of the binding affinity, it is important to consider possible rebinding effects, since they can influence the binding behaviour.

The main topic and structure of this thesis is based on Weber and Fackeldey[56], though with the addition of considering non-reversible processes as proposed by the same authors[54]. The mathematical foundations presented in the first two chapters are inspired by the book "Metastability and Markov State Models in Molecular Dynamics" by Schütte and Sarich[42]. Furthermore, the dissertations of Huisinga[21], Weber[52], Nielsen[30] and the habilitation of Weber[53] have been particularly useful for the deeper understanding of the mathematical concepts behind metastability, clustering and transfer operators.

Thesis Structure

Chapter 1 - Markov State Models

We give a short overview about Markov processes and how their evolution in time can be described by transition functions and transfer operators. We show how such a continuous operator can be projected onto a finite-dimensional space with the aid of a Galerkin discretization. Finally, we analyze the discretization error and the possible loss of the Markov property which can occur by this projection.

Chapter 2 - Dominant Structures

In order to create a suitable Markov State Model preserving the long-time behaviour of the original process, we introduce the concept of metastability. We define metastable sets mathematically and explain their relevance for molecular systems. We reveal their relation to the spectrum of the transfer operator and show that the "best" metastable decomposition is achieved in terms of fuzzy membership functions, which may be overlapping. Finally, we extend this well-established clustering method to non-reversible processes by employing the Schur decomposition.

Chapter 3 - Rebinding Effect

In this chapter, we characterize the rebinding effect as a memory effect which occurs in the context of receptor-ligand systems, a special case of molecular systems. We apply the methods presented in the first chapters in order to rigorously describe a molecular system respectively its projection onto a finite subspace. Finally, we compute a minimal bound for the rebinding effect as the solution of an optimization problem, for reversible as well as for non-reversible systems.

Chapter 4 - Illustrative Examples

The results from chapter 3 are verified by means of some illustrative examples. The minimal rebinding effect is first computed for some clusterings of a reversible system in order to evaluate the quality of this estimation. Afterwards, this system will be perturbed to non-reversibility and the outcome compared to the reversible case. Then, the rebinding effect is analyzed in a real-world application, describing the chemical reaction of a molecule. As the rebinding effect is characterized within receptor-ligand systems, such a system is examined as well.

1 Markov State Models

In order to be able to describe dynamical systems having a nondeterministic behaviour, we introduce Markov processes. They are memoryless stochastic processes which are commonly used to model different kinds of real-world processes. Recently they have been applied a lot in the research area of modelling biomolecular systems[36, 42]. As those systems are enormously large, it is very difficult to perform simulations on feasible time scales. That is why a reduction of complexity is needed. The originally large process is projected onto a suitable subspace, while maintaining the most relevant dynamical properties. We present such a reduced model, called "Markov State Model"[32].

In order to adequately define a Markov State Model, we first introduce some basic definitions and properties of stochastic processes and describe how their time-evolution can be characterized by a transfer operator. The actual dimension reduction of the process is realized by a Galerkin projection applied to the transfer operator. By that action, states of the original process are clustered conveniently.

1.1 Markov Process

Markov processes are a special type of stochastic processes and a generalization of the well-known Markov chains. Markov chains were defined as memoryless processes acting on finite state spaces and evolving in discrete time, a behaviour that can be represented by a stochastic matrix. For general Markov processes, both time and space can be continuous. Consequently, more extensive formulations and tools are required in order to rigorously describe such processes and their evolution in time.

Transition Function

We will denote by $E := (E, \Sigma)$ a *measurable space*, that is a set E with some σ-algebra Σ defined on it. The triple $\Omega := (\Omega, \mathcal{A}, \mathbb{P})$ will be a *probability space*, that is a measurable space with a probability measure $\mathbb{P}$ defined on it; more detailed information about these basic measure theoretic notations can be found in Bogachev[4, chapter 1].

A *random variable* $X : \Omega \to E$ is a *measurable function* from a probability space Ω into a measurable space E, meaning that preimages of measurable sets in E are measurable in Ω:

$$A \in \Sigma \Rightarrow X^{-1}(A) \in \mathcal{A}.$$

Then the probability measure $\mathbb{P}$ of Ω induces a canonical probability measure on E, by

$$\mu(A) := \mathbb{P}(X \in A) := \mathbb{P}(X^{-1}(A))$$

for all $A \in \Sigma$, called the *distribution* of X, see Øksendal[31, section 2.1].

Definition 1.1. (Stochastic process)
A family $(X_t)_{t\in\mathbb{T}}$ of random variables $X_t : \Omega \to E$ on some index set $\mathbb{T}$ is called a *stochastic process* on a state space E.

In the following, we consider stochastic processes on real state spaces $E \subset \mathbb{R}^d, d \in \mathbb{N}$, equipped with the Borel-σ-algebra $\Sigma = \mathcal{B}(E)$. In order to introduce Markov processes as a special type of stochastic processes, we need a tool to describe the time evolution of a process. This can be done using the transition function which describes the propagation of the distribution functions of a stochastic process.

Definition 1.2. (Transition function)
A function $p : \mathbb{T} \times E \times \Sigma \to [0, 1]$ is a *transition function* if it fulfills the following properties:

i) $x \mapsto p(t, x, A)$ is measurable on E for all $t \in \mathbb{T}$ and $A \in \Sigma$,

ii) $A \mapsto p(t, x, A)$ is a probability measure for all $t \in \mathbb{T}$ and $x \in E$,

iii) $p(0, x, E \setminus x) = 0$ for all $x \in E$,

iv) the Chapman-Kolmogorov equation

$$p(t + s, x, A) = \int_E p(t, x, \mathrm{d}z)p(s, z, A). \tag{1.1}$$

holds for all $t, s \in \mathbb{T}, x \in E$ and $A \in \Sigma$.

In this definition, the first three properties ensure that we get reasonable results and that the process can only be in one state at the same time. From the Chapman-Kolmogorov equation (1.1), it follows that the transition function $p(t, x, A)$ can be considered as the probability to get into a certain subset A in a time interval t starting from a point x. That means that we can describe the time evolution of a stochastic process by a transition function. In particular, the transition matrix of a Markov chain is a special case of the transition function since it fulfills the above properties.

Markov Process

Since the transition function comprises all possible transition probabilities between subsets of E, it enables us to define Markov processes.

Definition 1.3. (Markov Process)
A stochastic process $(X_t)_{t\in\mathbb{T}}$ on a state space E is a *Markov process* if its transition function fulfills the equation

$$p(t, x, A) = \mathbb{P}(X_{t+s} \in A \mid X_s = x). \tag{1.2}$$

for all $s, t \in \mathbb{T}$, $x \in E$ and $A \in \Sigma$. If that probability is independent from s, then the Markov process is called *time-homogeneous*.

We are especially interested in time-homogeneous processes, which will be presumed from now on. As we can see from the definition, all possible transition probabilities are given and hence, the time evolution of a Markov process is completely described by its transition function. Thus, a Markov process is uniquely determined by its transition function and an initial distribution μ. It is a process with "no memory" in the sense that only the last known state has an influence on the future of the process, as we can see on the right side of (1.2). Indeed, there is a one-to-one relation between transition functions and Markov processes, i.e. every homogeneous Markov process defines a transition function and vice versa, see Meyn and Tweedie[29, section 3.4]. The beginning of a Markov process X_t with the transition function p fulfills

$$\mathbb{P}_\mu(X_0 \in A, X_t \in B) = \int_A p(t, x, B)\mu(\mathrm{d}x) \tag{1.3}$$

for any $A, B \in \Sigma$, where $\mathbb{P}_\mu$ indicates that $X_0 \sim \mu$, or equivalently $\mu(A) = \mathbb{P}(X_0 \in A)$.

The transition function for a Markov process plays the same role as the transition matrix for a Markov chain; it propagates its distributions in time. If we choose $t = 1$ and transitions into one-elementic subsets, then the transition function corresponds to the 1-step transition matrix $[p_{ij}] = P \in \mathbb{R}^{n\times n}$ of a Markov chain. Having introduced the notion of Markov processes, we can define important properties and give some examples.

Invariant Measure

Definition 1.4. (Invariant measure)
Let $(X_t)_{t\in\mathbb{T}}$ be a Markov process. The probability measure μ is *invariant* with respect to $(X_t)_{t\in\mathbb{T}}$ if for all $t \in \mathbb{T}$ and $A \in \Sigma$ we have

$$\int_E p(t, x, A)\mu(\mathrm{d}x) = \mu(A).$$

In other words, a measure is invariant with respect to a Markov process if the probability to **be** in any subset of the state space is the same as the probability to **get** into that subset by the evolution of the Markov process for any fixed transition time. This means that the process is in "equilibrium" and does not change in time under this measure, which is also called a *stationary* measure for this reason.

Ergodicity

The long-time behaviour of stochastic processes can be described using ergodicity.

Definition 1.5. (Ergodic process)
Let $(X_t)_{t\in\mathbb{T}}$ be a Markov process with invariant probability measure μ. Then $(X_t)_{t\in\mathbb{T}}$ is *ergodic* with respect to μ if for all functions $u : E \to \mathbb{R}$ with $\int_E |u|\mu(\mathrm{d}x) < \infty$ we have

$$\lim_{T\to\infty} \frac{1}{T} \int_0^T u(X_t)\,\mathrm{d}t = \int_E u(x)\mu(\mathrm{d}x).$$

for almost all initial values $X_0 = x_0$.

In that sense, a Markov process is ergodic if its time average is the same as its average over the probability space. In an ergodic process, the state of the process after a long time is nearly independent of its initial state.

Reversibility

Reversibility describes the invariance of a process with respect to time-reversal. In the next section, we will see that operators describing reversible processes yield some very favorable properties, which makes them particularly easy to analyze.

Definition 1.6. (Reversible process)
Let $(X_t)_{t\in\mathbb{T}}$ be a Markov process with invariant probability measure μ. Then $(X_t)_{t\in\mathbb{T}}$ is *reversible* with respect to μ if

$$\int_A p(t,x,B)\mu(\mathrm{d}x) = \int_B p(t,x,A)\mu(\mathrm{d}x)$$

for all $t \in \mathbb{T}$ and $A, B \in \Sigma$. If μ is unique, then X_t is simply called *reversible*.

For a reversible process, the probability to get from any subset A to another subset B in a fixed time is the same as the probability for the reverse transition in the same time span. This definition implies that the process keeps the same probability law even if its movement is considered backwards in time.

Example: Markov Chain

Let $(X_t)_{t\in\mathbb{T}}$ be a Markov chain on discrete time $\mathbb{T} = \mathbb{N}$ and finite state space $E = \{1, \ldots, n\}$. Since we consider 1-step transitions, the associated transition function is given by $p(x,y) := p(1,x,y)$ and corresponds to the entries of the *transition matrix* $P \in \mathbb{R}^{n\times n}$, that is

$$P_{xy} = p(x,y) = \mathbb{P}(X_1 = y \mid X_0 = x).$$

The propagation of a probability distribution $v_0 \in \mathbb{R}^n$ in the state space can be written as $v_1^T = v_0^T P$, where v_0^T denotes the transposed vector of v_0. The invariant measure is given by the stationary distribution $\pi \in \mathbb{R}^n$, a normalized positive vector satisfying $\pi^T = \pi^T P$. If P is irreducible, such an eigenvector exists due to Perron-Frobenius theorem[20, P7.3.5] and in this case, the corresponding eigenvalue 1 is simple.

Reversibility of a Markov chain can be characterized by the *detailed balance condition*

$$\pi_i \cdot \mathbb{P}(X_1 = j \mid X_0 = i) = \pi_j \cdot \mathbb{P}(X_1 = i \mid X_0 = j) \quad \forall i,j \in E.$$

A more compact way to write this equation uses the diagonal matrix $D = \mathrm{diag}(\pi_1, \ldots, \pi_n)$. Then a Markov chain is reversible if and only if its transition matrix P fulfills

$$DP = P^T D. \tag{1.4}$$

1.2 Transfer Operator

With the previously defined transition function, we have a tool to describe the propagation of distributions of stochastic processes. Based on that, we define a transfer operator propagating probability densities of Markov processes, as introduced by Schütte et al[41]. Before defining such an operator, we have to specify the space of functions the operator is acting on.

L^r-Spaces

It seems natural to define such a density propagating operator as acting on $L^1(\mu)$, the Banach space that includes all probability densities with respect to μ. However, it is sometimes advantageous to restrict the analysis to $L^2(\mu)$, since this may yield a self-adjoint operator. As there are different motivations for the choice of a suitable space, we define an operator which acts on $L^r(\mu)$-spaces, i.e. spaces of r-integrable functions.

Definition 1.7. (L^r-Spaces)
Let (E, Σ, μ) be a probability space. The corresponding L^r-spaces are defined as equivalence classes of measurable functions

$$L^r(E, \Sigma, \mu) = \{f : E \to \mathbb{R} \mid \int_E |f(x)|^r \mu(\mathrm{d}x) < \infty\}$$

for $1 \leq r < \infty$ and

$$L^\infty(E, \Sigma, \mu) = \{f : E \to \mathbb{R} \mid \operatorname*{ess\,sup}_{x \in E} |f(x)|^r \mu(\mathrm{d}x) < \infty\},$$

with the corresponding norms $\|\cdot\|_r$ and $\|\cdot\|_\infty$, respectively.

In these equivalence classes, two functions f and g are identified if $f = g$ μ-almost everywhere, see Werner[58, section I.1]. If it is clear from the context, which probability space (E, Σ, μ) is in consideration, we just write shortly $L^r(\mu) := L^r(E, \Sigma, \mu)$. Due to Hölders inequality, we have $L^r(\mu) \subset L^s(\mu)$ for all $1 \leq s \leq r \leq \infty$. All L^r-spaces are Banach spaces, though $L^2(\mu)$ is the only one which can be equipped with a canonical scalar product and thereby becomes a Hilbert space, see Werner[58, section V.1]. For $f, g \in L^2(\mu)$, the scalar product is defined as

$$\langle f, g \rangle_\mu := \int_E f(x) g(x) \mu(\mathrm{d}x).$$

Now let ν_0 be the density function of a given start distribution. Then the density function of a subset $A \in \Sigma$ at time t is given in terms of the transition function by

$$\nu_t(A) = \int_E \nu_0 p(t, x, A) \mu(\mathrm{d}x).$$

On the other hand, the density ν_t is given by

$$\nu_t(A) = \int_A \nu_t(x) \mu(\mathrm{d}x).$$

Forward and Backward Transfer Operator

The two above equations result in the following definition of a transfer operator which should "propagate" probability densities according to a given Markov process. But instead of limiting us to density functions, we define the transfer operator as acting on any r-integrable function.

Definition 1.8. (Propagator or Forward Transfer Operator)
Let $p : \mathbb{T} \times E \times \Sigma \to [0, 1]$ be the transition function of a Markov Process $(X_t)_{t\in\mathbb{T}}$ with an invariant measure μ. The set of *propagators* or *forward transfer operators* $\mathcal{T}^t : L^r(\mu) \to L^r(\mu)$ with $t \in \mathbb{T}$ and $1 \leq r \leq \infty$ is defined via

$$\int_A \mathcal{T}^t \nu(y)\mu(\mathrm{d}y) = \int_E \nu(x)p(t, x, A)\mu(\mathrm{d}x) \tag{1.5}$$

for all $A \in \Sigma$ and $\nu \in L^r(\mu)$.

The propagator[1] $\mathcal{T}$ is well-defined on the Banach spaces $L^r(\mu)$, $1 \leq r \leq \infty$, see Huisinga[21]. $\mathcal{T}^t\nu_0$ describes the transport of the function ν_0 in time t by the underlying dynamics given by the process X_t and weighted with respect to μ via

$$\nu_0 \mapsto \nu_t = \mathcal{T}^t\nu_0.$$

Since μ is invariant, we immediately see that the characteristic function $\mathbb{1} := \mathbb{1}_E$ of the entire state space is invariant under the action of $\mathcal{T}$, that is

$$\mathcal{T}\mathbb{1} = \mathbb{1}.$$

It means that $\mathcal{T}$ has the eigenvalue 1 corresponding to the eigenfunction $\mathbb{1}$.

Definition 1.9. (Backward Transfer Operator)
The *backward transfer operator* $\mathcal{P}^t : L^r(\mu) \to L^r(\mu)$ with $t \in \mathbb{T}$ and $1 \leq r \leq \infty$ is defined by

$$\mathcal{P}^t f(x) = \int_E f(y)p(t, x, \mathrm{d}y). \tag{1.6}$$

For this operator as well, we obtain 1 as eigenvalue to the eigenfunction $\mathbb{1}$, that is

$$\mathcal{P}\mathbb{1} = \mathbb{1}.$$

Both operators $\mathcal{P}$ and $\mathcal{T}$ conserve the norm $\|\mathcal{P}f\|_1 = \|f\|_1$ and are positive, $\mathcal{P}f \geq 0$ for $f \geq 0$, see Schütte and Sarich[42]. If we compare the equations (1.5) and (1.6), the notion of "forward" and "backward" becomes clear. For the forward transfer operator, the state average with respect to a function is taken over all initial states x which are propagated forward in time, whereas for the backward transfer operator, we take the state average over all final states y.

[1] If the lag-time t is not of importance, e.g. if a property is valid for all t, then we omit it and write $\mathcal{T} := \mathcal{T}^t$.

The operator $\mathcal{P}^t$ is *adjoint* to $\mathcal{T}^t$, denoted by $(\mathcal{T}^t)^* = \mathcal{P}^t$, i.e. they are related via

$$\langle \mathcal{T}^t f, g\rangle_\mu = \langle f, \mathcal{P}^t g\rangle_\mu, \tag{1.7}$$

for all $f \in L^p(\mu), g \in L^q(\mu)$ with $\frac{1}{p} + \frac{1}{q}$. In order to obtain this useful adjointness-relation, it is reasonable to restrict these operators to act on $L^2(\mu)$ and $L^2(\mu)$ respectively $L^1(\mu)$ and $L^\infty(\mu)$.

In the further course of this thesis, we will be concerned with the backward transfer operator and just call it "transfer operator". However, because of this adjointness, many properties of the two transfer operators coincide. The actual conceptual connection between them becomes more comprehensible by considering their finite versions in the next section. A deeper analysis of both transfer operators and their relation can be found in Nielsen[30].

Spectrum of Transfer Operator

Later in this thesis, we will be interested in examining the spectrum of the transfer operator of a given Markov process. The following theorems give us an important insight about the spectrum and its relation to the reversibility of the process.

Definition 1.10. (Self-adjoint Operator)
An operator $\mathcal{U}$ on $L^2(\mu)$ is called *self-adjoint* if for all $f, g \in L^2(\mu)$ we have

$$\langle f, \mathcal{U} g\rangle_\mu = \langle \mathcal{U} f, g\rangle_\mu.$$

Theorem 1.11. (Werner[58, Theorem VI.1.2, Theorem VI.1.3, Lemma VI.3.1])
Let X be a Banach space and $\mathcal{U} : X \to X$ a linear continuous operator. Then

$$|\lambda| \leq \|\mathcal{U}\| \quad \textit{for all} \quad \lambda \in \sigma(\mathcal{U}).$$

If X is additionally a Hilbert space, then

i) $\sigma(\mathcal{U}^*) = \{\bar{\lambda} \mid \lambda \in \sigma(\mathcal{U})\}$,

ii) if $\mathcal{U}$ is self-adjoint, then $\sigma(\mathcal{U}) \subset \mathbb{R}$,

iii) if $\mathcal{U}$ is self-adjoint, then each two eigenfunctions corresponding to different eigenvalues are orthogonal.

Since we know that the operator norm of any transfer operator $\mathcal{P}$ is 1, it follows immediately from theorem 1.11 that the spectrum $\sigma(\mathcal{P})$ is contained in the unit circle of the complex plane, that is we have $|\lambda| \leq 1$ for all $\lambda \in \sigma(\mathcal{P}) \subset \mathbb{C}$.

Theorem 1.12. (Huisinga[21, Proposition 1.1])
Let $\mathcal{P} : L^2(\mu) \subset L^1(\mu) \to L^2(\mu)$ be the transfer operator corresponding to the Markov process $(X_t)_{t\in\mathbb{T}}$. Then $\mathcal{P}$ is self-adjoint with repect to the scalar product $\langle\cdot,\cdot\rangle_\mu$ in $L^2(\mu)$ if and only if $(X_t)_{t\in\mathbb{T}}$ is reversible.

It follows that the transfer operator of a reversible process has a real spectrum $\sigma(\mathcal{P}) \subset [-1, 1]$, a property that will be very advantageous for the later investigations.

Infinitesimal Generator

For $\mathbb{T} = \mathbb{R}$ the Chapman-Kolmogorov property (1.1) of the transition functions makes the family $\{\mathcal{P}^t\}_{t\in\mathbb{R}}$ of corresponding transfer operators a continuous *semigroup* due to

$$\mathcal{P}^{t+s} = \mathcal{P}^t \mathcal{P}^s.$$

A proof for the forward as well as for the backward transfer operator can be found in Schütte and Sarich[42, appendix A]. This leads to the following definition of the time-independent infinitesimal generator.

Definition 1.13. (Infinitesimal Generator)
For the semigroup of transfer operators $\mathcal{P}^t : L^r(\mu) \to L^r(\mu)$ with $t \in \mathbb{T}$ and $1 \le r \le \infty$ we define $\mathcal{D}(\mathcal{Q})$ as the set of all $f \in L^r(\mu)$ such that the strong limit

$$\mathcal{Q}f = \lim_{t\to 0} \frac{\mathcal{P}^t f - f}{t}$$

exists. Then the operator $\mathcal{Q} : \mathcal{D}(\mathcal{Q}) \to L^r(\mu)$ is called the *infinitesimal generator* of $\mathcal{P}^t$.

The infinitesimal generator is an operator which describes the behaviour of a Markov process in infinitesimal time. That becomes clear by the relation

$$\mathcal{P}^t = \exp(t\mathcal{Q}) \tag{1.8}$$

in $L^2(\mu)$, see [42], which implies that $\mathcal{Q}$ "generates" the semigroup of transfer operators $\{\mathcal{P}_t\}_{t\in\mathbb{R}}$. The whole semi-group of transfer operators can be derived from it, by choosing the desired lag-time t and computing the corresponding transfer operator with (1.8). If the associated Markov process is reversible, then $\mathcal{Q}$ is self-adjoint in $L^2(\mu)$ and the spectrum is contained in $(-\infty, 0]$, which can easily deduced from theorems 1.11 and 1.12. Consequently, the dominant eigenvalues $1 = \lambda_1, \ldots, \lambda_n$ of the transfer operator $\mathcal{P}^t$ are related to the dominant eigenvalues $0 = \xi_1, \ldots, \xi_n$ of the generator $\mathcal{Q}$ via

$$\lambda_i = \exp(t\xi_i)$$

for all $1 \le i \le n$ and the associated eigenfunctions are identical. Thus, the eigenfunction $\mathbb{1}$ of $\mathcal{P}$ is as well an eigenfunction for $\mathcal{Q}$ to the dominant eigenvalue $\xi_1 = 0$, satisfying

$$\mathcal{Q}\mathbb{1} = 0,$$

where 0 is the constant zero function on E.

1.3 Galerkin Projection

So far we considered Markov processes on very large, possibly continuous, state spaces. For many applications, simulations of a given process are needed in order to obtain informations about the system, though computations on large state spaces require an enormous amount of computation power and time. With enlarging the state space, the computation effort increases exponentially fast, see "curse of dimensionality" [3]. For that reason, we are interested in reducing the number of states in order to be able to perform computations on reasonable time-scales. Such a reduction can be realized by a projection. In this section, we present the mathematical concept which enables us to create such a reduced model.

Galerkin Projection

The first step in order to create a finite process is to determine a convenient finite state space $D \subset L^2(\mu)$. For this purpose, we choose a partition of unity as a basis, which is a generalization of a set of characteristic functions. This more general idea gives us more flexibility for later applications. The relevance of this choice for the projection will be clarified in section 2.3.

Definition 1.14. (Partition of Unity)
A family of measurable functions $\{\chi_1, \dots, \chi_n\} : E \to [0, 1]$ in $L^2(\mu)$ is called a *partition of unity* if the following two conditions are fulfilled:

i) The χ_i are non-negative and linear independent.

ii) $\sum_{i=1}^{n} \chi_i(x) = 1$ for all $x \in E$.

Definition 1.15. (Galerkin Projection)
Let $\{\chi_1, \dots, \chi_n\}$ be a partition of unity, $D = \text{span}\{\chi_1, \dots, \chi_n\}$ the associated finite-dimensional ansatz space and $\hat{S} \in \mathbb{R}^{n \times n}$ with $\hat{S}_{kj} = \langle \chi_k, \chi_j \rangle_\mu$. The *Galerkin projection* onto D is defined by $G : L^2(\mu) \to D$ via

$$Gf = \sum_{k,j=1}^{n} (\hat{S}^{-1})_{kj} \langle \chi_k, f \rangle_\mu \chi_j. \tag{1.9}$$

The matrix $\hat{S}$ is invertible since it is the Gramian matrix of linear independent functions. In the easy case that the $\{\chi_1, \dots, \chi_n\}$ are the characteristic functions $\{\mathbb{1}_{A_1}, \dots, \mathbb{1}_{A_n}\}$ belonging to a full partition $\{A_1, \dots, A_n\}$, equation (1.9) becomes

$$Gf = \sum_{k=1}^{n} \frac{1}{\mu(A_k)} \langle \chi_k, f \rangle_\mu \chi_k,$$

since the χ_i are orthogonal which means that $\chi_k \chi_j = 1$ if $j = k$ and 0 otherwise. A Galerkin projection can be applied on the transfer operator of a Markov process as well.

Definition 1.16. (Projected Transfer Operator)
Let $\mathcal{P}$ be the transfer operator of a Markov process on a state space E with unique invariant measure μ, $\{\chi_1, \ldots, \chi_n\}$ be a partition of unity and G the Galerkin projection onto the associated subspace D. Then an operator of the form

$$G\mathcal{P}G : L^2(\mu) \to D$$

is called *projected transfer operator* and we abbreviate it by $G(\mathcal{P})$.

Matrix Representation

We want to propagate n-dimensional vectors by the projected transfer operator. For this reason, we consider the projection of the restricted transfer operator $G\mathcal{P}_{|D} : D \to D$, denoted by $G(\mathcal{P})$ as well. Every linear map between finite-dimensional vector spaces can be represented by a matrix which is determined by chosen bases. Accordingly, we can write the projected transfer operator as a $n \times n$-matrix in the following useful way.

Theorem 1.17. *Let $\mathcal{P}$ be the transfer operator of a Markov process, $\{\chi_1, \ldots, \chi_n\}$ a partition of unity and $G(\mathcal{P})$ the Galerkin projection of the transfer operator onto the associated subspace. Then $G(\mathcal{P})$ has a matrix representation*

$$P_c = S^{-1}T,$$

with

$$T_{kj} = \frac{\langle \chi_k, \mathcal{P}\chi_j \rangle_\mu}{\langle \chi_k, \mathbb{1} \rangle_\mu} \quad \text{and} \quad S_{kj} = \frac{\langle \chi_k, \chi_j \rangle_\mu}{\langle \chi_k, \mathbb{1} \rangle_\mu}. \tag{1.10}$$

Proof. Remember that P_c is a (right) matrix representation of $G(\mathcal{P})$ with respect to a basis $\{\psi_1, \ldots, \psi_n\}$ of D if for any function $f : D \to D$ with

$$f = \sum_{i=1}^{n} \alpha_i \psi_i \quad \text{and} \quad G(\mathcal{P})f = \sum_{i=1}^{n} \beta_i \psi_i \tag{1.11}$$

it holds that

$$P_c(\alpha_1, \ldots, \alpha_n)^T = (\beta_1, \ldots, \beta_n)^T, \tag{1.12}$$

or equivalently $\beta_l = \sum_{k=1}^{n} \alpha_k (P_c)_{lk}$. Assuming that (1.11) is true, we aim to show (1.12). For that purpose, we choose a basis $\{\psi_1, \ldots, \psi_n\}$ of D with

$$\psi_k = \chi_k. \tag{1.13}$$

As $G(\mathcal{P})$ is a linear map, we have $G(\mathcal{P})f = \sum \alpha_i G(\mathcal{P})\psi_i$. We exploit this fact, as well as the definitions of the Galerkin projection and the basis to compute

$$\begin{aligned}
G(\mathcal{P})f &= \sum_{k=1}^{n} \alpha_k G(\mathcal{P})\psi_k \\
&\overset{(1.9)}{=} \sum_{k,l,j=1}^{n} \alpha_k (\hat{S}^{-1})_{jl} \langle \chi_j, \mathcal{P}\psi_k \rangle_\mu \chi_l \\
&\overset{(1.13)}{=} \sum_{k,l,j=1}^{n} \alpha_k (\hat{S}^{-1})_{jl} \langle \chi_j, \mathcal{P}\psi_k \rangle_\mu \psi_l \\
&\overset{(1.11)}{=} \sum_{l=1}^{n} \beta_l \psi_l .
\end{aligned}$$

Comparing the coefficients of the last two equations, we can express β_l as

$$\begin{aligned}
\beta_l &= \sum_{k,j=1}^{n} \alpha_k (\hat{S}^{-1})_{jl} \langle \chi_j, \mathcal{P}\psi_k \rangle_\mu \\
&= \sum_{k=1}^{n} \alpha_k \underbrace{\sum_{j=1}^{n} (\hat{S}^{-1})_{jl} \langle \chi_j, \mathcal{P}\chi_k \rangle_\mu}_{\overset{!}{=}(P_c)_{lk}} . \qquad (1.14)
\end{aligned}$$

The underbraced term **should** be equal to $(P_c)_{lk}$ because we wish that (1.12) is fulfilled. Thus, we compute the (l,k)-th entry of $P_c = S^{-1}T$, employing $(S^{-1})_{lj} = (\hat{S}^{-1})_{lj}\langle \chi_j, \mathbb{1}\rangle$, as

$$\begin{aligned}
(S^{-1}T)_{lk} &= \sum_{j=1}^{n} (S^{-1})_{lj} T_{jk} \\
&= \sum_{j=1}^{n} (\hat{S}^{-1})_{lj} \langle \chi_j, \mathbb{1}\rangle_\mu \frac{\langle \chi_j, \mathcal{P}\chi_k \rangle_\mu}{\langle \chi_j, \mathbb{1}\rangle_\mu} \\
&= \sum_{j=1}^{n} (\hat{S}^{-1})_{lj} \langle \chi_j, \mathcal{P}\chi_k \rangle_\mu
\end{aligned}$$

and discover that it is equal to the underbraced term in (1.14), since $\hat{S}$ is symmetric. Hence, (1.12) is true and consequently P_c is the requested matrix representation of $G(\mathcal{P})$. □

The proof of theorem 1.17 has been conducted similar to Schütte and Sarich[42, chapter 5]. They proved an analogous statement for the forward transfer operator $\mathcal{T}$, yielding a left matrix representation TS^{-1}, employing a normalized basis $\psi_k = \chi_k / \langle \chi_k, \mathbb{1}\rangle$. These two matrices are the transposed of each other, which can be explained as follows: each matrix can be interpreted as representing two linear maps - by left and right multiplication with a vector. If we consider P_c as a row-stochastic matrix, then it propagates a probability distribution v_0 by multiplication $v_0^T P_c$ from the left, while it computes probabilities to reach a subset A via

$P_c\mathbb{1}_A$ by multiplication with a characteristic vector from the right. The first map corresponds to the forward transfer operator $\mathcal{T}$, the latter corresponds to the backward transfer operator $\mathcal{P}$. Consequently, the projection P_c can be interpreted as a unified matrix representation for both transfer operators. That is plausible since they describe the stochastical behaviour of the same Markov process $(X_t)_{t\in\mathbb{T}}$, encoded in the transition function $p(t,x,A)$.

Theorem 1.18. *The matrices S and T from theorem 1.17 are stochastic.*

Proof. In order to be stochastic, each row must sum up to 1. We exploit the partition of unity property $\sum_j \chi_j = 1$ and $\mathcal{P}\mathbb{1} = \mathbb{1}$ to obtain

$$\sum_{j=1}^n S_{kj} = \frac{\langle \chi_k, \sum_j \chi_j\rangle_\mu}{\langle \chi_k, \mathbb{1}\rangle_\mu} = \frac{\langle \chi_k, \mathbb{1}\rangle_\mu}{\langle \chi_k, \mathbb{1}\rangle_\mu} = 1,$$

$$\sum_{j=1}^n T_{kj} = \frac{\langle \chi_k, \sum_j \mathcal{P}\chi_j\rangle_\mu}{\langle \chi_k, \mathbb{1}\rangle_\mu} = \frac{\langle \chi_k, \mathcal{P}\mathbb{1}\rangle_\mu}{\langle \chi_k, \mathbb{1}\rangle_\mu} = \frac{\langle \chi_k, \mathbb{1}\rangle_\mu}{\langle \chi_k, \mathbb{1}\rangle_\mu} = 1.$$

Non-negativity follows from the non-negativity of the $\{\chi_1, \dots, \chi_n\}$. □

Since both S and T are stochastic, they have the constant vector $e = (1, \dots, 1)^T$ as right eigenvector to the eigenvalue 1. The same holds for P_c, i.e. its rows sum up to 1 and thus the product $S^{-1}T$ is at least pseudostochastic. However, non-negativity is not assured since inverting S can provoke negative entries. The non-negativity depends on the choice of the partition of unity.

Theorem 1.19. *The matrix representation P_c from theorem 1.17 has the left eigenvector $\hat{\mu} \in D$ with the entries*

$$\hat{\mu}_j = \langle \mathbb{1}, \chi_j\rangle_\mu = \int_E \chi_j(x)\mu(\mathrm{d}x).$$

Proof. We observe that $\hat{\mu}^T S = \hat{\mu}^T$ and $\hat{\mu}^T T = \hat{\mu}^T$ since

$$(\hat{\mu}^T S)_j = \sum_{k=1}^n \langle \mathbb{1}, \chi_k\rangle_\mu \frac{\langle \chi_k, \chi_j\rangle_\mu}{\langle \chi_k, \mathbb{1}\rangle_\mu} = \langle \mathbb{1}, \chi_j\rangle_\mu = \hat{\mu}_j$$

and

$$(\hat{\mu}^T T)_j = \sum_{k=1}^n \langle \chi_k, \mathcal{P}\chi_j\rangle_\mu = \langle \mathbb{1}, \mathcal{P}\chi_j\rangle_\mu \overset{(1.7)}{=} \langle \mathcal{T}\mathbb{1}, \chi_j\rangle_\mu = \langle \mathbb{1}, \chi_j\rangle_\mu = \hat{\mu}_j.$$

We can deduce that $\hat{\mu}^T P_c = \hat{\mu}^T S^{-1} T = \hat{\mu}^T S S^{-1} T = \hat{\mu}^T T = \hat{\mu}^T$. □

The eigenvalue $\lambda = 1$ of P_c has the associated right-eigenvector $e = (1, \dots, 1)^T$ and left-eigenvector $\hat{\mu}^T$. If the transfer operator has a simple and dominant eigenvalue 1 and the continuous part of the spectrum is bounded away from the discrete part, then the process is irreducible and aperiodic which is inherited by the matrix T. In particular T has the simple and dominant eigenvalue $\lambda = 1$ which is the only eigenvalue with $|\lambda| = 1$ and the discrete invariant density $\hat{\mu}$ is the unique invariant density of T, see [42].

Example: Full Partition Discretization

Let $A_1, \ldots, A_n$ be a partition of the state space E, i.e. they are pairwise disjoint sets such that $\cup A_i = E$. We consider the family of the corresponding characteristic functions

$$\chi_i(x) = \mathbb{1}_{A_i}(x).$$

Since they are orthogonal, the matrix S is the identity matrix and therefore, the matrix representation of the Galerkin projection is $P_c = T$. We can compute it by combining

$$\langle \mathbb{1}_{A_i}, \mathcal{P}\mathbb{1}_{A_j} \rangle_\mu = \int_{A_i} (\mathcal{P}\mathbb{1}_{A_j})(x)\mu(\mathrm{d}x) \overset{(1.6)}{=} \int_{A_i} p(t, x, A_j)\mu(\mathrm{d}x) \overset{(1.3)}{=} \mathbb{P}_\mu(X_t \in A_j, X_0 \in A_i)$$

and

$$\langle \mathbb{1}_{A_i}, \mathbb{1} \rangle_\mu = \int_E \mathbb{1}_{A_i}(x)\mu(\mathrm{d}x) = \mu(A_i) = \mathbb{P}_\mu(X_0 \in A_i).$$

The entries of the resulting matrix representation are given by

$$T_{ij} = \frac{\langle \mathbb{1}_{A_i}, \mathcal{P}\mathbb{1}_{A_j} \rangle_\mu}{\langle \mathbb{1}_{A_i}, \mathbb{1} \rangle_\mu} = \mathbb{P}_\mu(X_t \in A_j \mid X_0 \in A_i).$$

Thus, P_c is a Markov chain on the partition sets A_i, i.e. each state of the projected process represents one of the A_i. The stationary distribution $\hat{\mu}$ of this Markov chain P_c is just the projection of the invariant measure μ onto $\{A_1, \ldots, A_n\}$ with the entries $\hat{\mu}_i = \mu(A_i)$ corresponding to the stochastic "weights" of the partition sets.

According to their definitions, the matrix T represents the dynamical behaviour of the original process $\mathcal{P}$, while the matrix S merely contains informations about the partition of unity, i.e. the basis of the clustering. For that reason, T is also called "coupling matrix" as it describes how the clustered subsets are interacting. This is particularly visible in the example of a full-partition decomposition, where the entries of T correspond to the transition probabilities between the clustered states, while S has no influence. However, the further S deviates from the identity matrix, the more it contributes to the projection P_c. The actual influence of S and its meaning for the clustered system will be of high interest and elaborated in chapter 2.

Projected Infinitesimal Generator

The Galerkin projection of an infinitesimal generator yields a similar matrix representation as the transfer operator. It can also be written as the product of two stochastic matrices, one of them being the inverted mass matrix of the partition of unity functions.

Theorem 1.20. (Schütte and Sarich[42])
Let $\mathcal{Q} : L^2(\mu) \to L^2(\mu)$ be the generator of a semigroup of transfer operators with unique invariant measure μ and satisfying $\mathcal{Q}\mathbb{1} = 0$. Let χ be a partition of unity with a projection G onto the associated subspace spanned by χ. Then the projected generator $G(\mathcal{Q})$ has the matrix representation $Q_c = S^{-1}R$ with the stochastic mass matrix S from (1.10) *and*

$$R(k,j) = \frac{\langle \chi_k, \mathcal{Q}\chi_j \rangle_\mu}{\langle \chi_k, \mathbb{1} \rangle_\mu}.$$

For both Q_c and R the largest eigenvalue is $\lambda = 0$. The associated right eigenvector is $e = (1, \ldots, 1)^T$ and the associated left eigenvector is $\hat{\mu}^T$ from theorem 1.19.

The proof is similar to theorem 1.17. There exist obviously many possible Galerkin projections for a given transfer operator or infinitesimal generator. We showed the example of a full-partition discretization, yielding a matrix representation $P_c = T$ with no contribution of S. As arbitrary partitions of unity $\chi_1, \ldots, \chi_n$ are allowed, there will be differing results, which require a further analysis of the matrices S and T. In chapter 2, we will see which choice of χ results in a good discretization in the sense that it represents the correct long-time behaviour of the process in terms of so called metastability.

1.4 Recrossing Effect

Concluding the first chapter, we give a short outlook about the so called recrossing effect, being closely related to the main topic of this thesis, the rebinding effect, which will be introduced in chapter 3. Furthermore, we explain how the quality of a Markov State Model can be measured by examining the iteration error.

Initial Situation

Assume we are given a Markov process $(X_t)_{t \in \mathbb{T}}$ on a continuous or very large state space E, described by the transfer operator $\mathcal{P} := \mathcal{P}(\tau)$. In order to get a discrete process out of it, we project the time onto $\mathbb{N}$ and the state space onto a finite set $\{1, \ldots, n\}$. Discretizing the time can be done naturally without problems since for every lag-time $\tau > 0$, the process $(X_{k\tau})_{k \in \mathbb{N}}$ is again Markovian.

However, the state-space discretization has to be observed a bit more elaborated. We do this on the example of a full partition discretization. We consider the operator $G(\mathcal{P}^k)$, that is we first propagate the process and project it afterwards. Then for all k-multiples of τ, we assign the partition set belonging to the current state of X_t to the projected process $\widetilde{X}_k$:

$$\widetilde{X}_k = i \Leftrightarrow X_{k\tau} \in A_i.$$

The process $\widetilde{X}_k$ describes the *snapshot dynamics* of X_t with lag time τ between the partition sets $A_1, \ldots, A_n$. This process is not necessarily Markovian, since $(G(\mathcal{P}^k))_k$ is in general not a semigroup, see Schütte and Sarich[42].

Recrossing in a Double Well Potential

Let X_t be the Markov process corresponding to the double-well potential $V(x) = (x^2 - 1)^2$. We consider a full-partition of the state space into two sets A and B around the local minima of the energy landscape, as shown in figure 1.1. We are interested if the induced process $\widetilde{X}_k$ inherits the Markovianity of X_t or if it contains any memory effects.

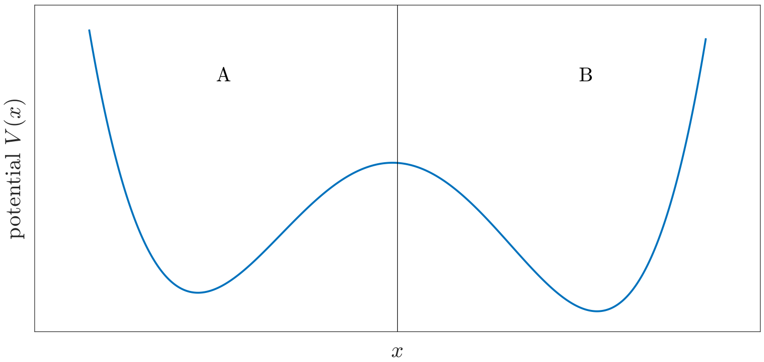

Figure 1.1: Full-partition of a double-well potential

For a small lag-time $\tau = 0.1$ we consider the probability of $\widetilde{X}_k$ to make a transition from B to A in one time-step and compare it to the probability of the same transition with the **additional** information of having been in A one time-step before. If the process was Markovian, then this additional information about the past should make no difference and consequently, both probabilities should be equal. However, the following two probabilities

$$\mathbb{P}_\mu[X_{(k+1)\tau} \in A \mid X_{k\tau} \in B], \tag{1.15}$$

$$\mathbb{P}_\mu[X_{(k+1)\tau} \in A \mid X_{k\tau} \in B, X_{(k-1)\tau} \in A]. \tag{1.16}$$

are different, which has been shown by Sarich[35, chapter 2]. For such a short lag-time τ, the process $\widetilde{X}_k$ is **not** independent of the past and hence **not** a Markov process. Equation (1.15) describes the probability to get from B to A, where "being in B" could mean everything from "close to the transition region" to "far away from the transition region". This probability is averaged over **all** possible starting points in B, since the spatial arrangement inside of B is not included in this reduced model. We compare it to (1.16), where having been in A shortly before being in B **increases** the probability to return to A again. This behaviour can be interpreted such that for a short time after a transition, the process is still likely to be inside of the transition region. In this example, the transition region is the area close to the maximum of potential energy. Thus, there still is an increased probability to return to the previous state, because of the spatial situation shortly after the transition.

This issue is called the *recrossing effect*, since additional memory leads to an increased probability to "recross" the energy barrier shortly after a transition. On the other hand, if we choose a large lag-time, e.g. $\tau = 100$, then the past transition from A to B in (1.16) took place a long time ago. In that case, the probability of the process to still be in the critical transition region is reduced; during that long lag-time it also could have moved anywhere else. This means that the memory effect included in $\widetilde{X}_k$ diminishes for larger lag-times and consequently can be considered as a "short-time memory".

Quality of Markov State Model

After having observed the recrossing effect as a memory effect occurring when projecting the time-series of a continuous process onto a finite subspace, we want to compare that result to the corresponding Markov State Model. So far, we considered the process $\widetilde{X}_k$ belonging to the operator $G(\mathcal{P}^k)$. Let $(\widehat{X}_k)_{k\in\mathbb{N}}$ be the Markov chain that is described by the transition matrix P_c, i.e. the matrix representation of the discretized transfer operator $G(\mathcal{P})$. Then the quality of the Markov State Model can be measured by considering the *iteration error*, i.e. the deviation of $(P_c)^k$ from the projected time-series for the same time-step. More clearly, we are interested if the Markov State Model behaves equally to the original process, represented by the projected time-series.

The iteration error of $P_c(\tau)$ is zero if the Galerkin projection of $(\mathcal{P}(\tau))^k$ is equal to the iteration $(P_c(\tau))^k$. That is the case if the actions of iteration and projection are commutative, i.e. if diagram 1.2 commutes. Then, it does not matter if we project the propagated process or if we propagate the projected process.

$$\begin{tikzcd} \mathcal{P}(\tau) \arrow[r, "\tau \to \tau k"] \arrow[d] & (\mathcal{P}(\tau))^k \arrow[d] \\ P_c(\tau) \arrow[r, "\tau \to \tau k"] & (P_c(\tau))^k \end{tikzcd}$$

Figure 1.2: Projecting and propagating a transfer operator.

In general, this diagram is **not** commutative and hence, in general we have

$$G(\mathcal{P}^k) \neq (P_c)^k.$$

Consequently, we have to distinguish between two kind of "errors" that can occur:

- Rebinding Events: Projection of time-series can include some kind of memory effect,
- Iteration Error: Deviation of $G(\mathcal{P}^k)$ and $(G(\mathcal{P}))^k$.

In order to work with a "correct" model, we aim at minimizing the iteration error. There exist upper bounds for this deviation by Sarich[35], indicating that the iteration error ceases for more iteration steps. We will not go into further details about it, since in chapter 2, we will present a projection under which this iteration error vanishes and the diagram in figure 1.2 commutes. However, despite not having to deal with an iteration error, the recrossing effect can occur and will be examined in chapter 3 in a different context.

2 Dominant Structures

With the Galerkin discretization, we introduced a method to reduce the dimension of a Markov process by projecting it onto a smaller state space. However, we did not yet specify how to choose a partition of unity such that this projection yields a reasonable Markov State Model, in the sense that important properties of the original process are maintained. The long-time behaviour of a process, which usually is of particular interest, is often determined by so called **metastabilities**. We explain why it makes sense to project a process onto its metastable sets and, in order to detect them, analyze their relation to the dominant spectrum of the transfer operator. Abandoning the non-overlapping approach, we demonstrate that the optimal metastable decomposition is rather fuzzy than crisp.

Additionally, we introduce a rather new concept to create a Markov State Model with the aid of a Schur decomposition. In contrast to the spectral approach, it includes nonreversible processes and provides some additional advantages, such as being able to identify different kinds of dominant structures.

2.1 Metastability

There exist several definitions of metastability. Shortly said, metastability is the property of a process to act on particular regions such that transitions between these regions are rare events while the duration of stay inside of each of them is comparatively long. Some possible characterizations of that behaviour are based on large hitting times or small exit rates, see Schütte and Sarich[42, chapter 3], where a good overview of the most common definitions can be found.

Mathematical Concept of Metastability

In order to describe the concept of metastability, it is a good way to start with so called *stable* or *invariant subsets*. A measurable subset $A \subset E$ of the state space of a Markov process X_t is called stable or invariant if it cannot be left, i.e. if $\mathbb{P}(X_t \in A \mid X_0 \in A) = 1$ for all t. Analogously, we can define a *metastable* or *almost invariant subset* as a subset in which the process will stay for a very long time before exiting it into any other subset, that is $\mathbb{P}(X_{t_f} \in A \mid X_0 \in A) \approx 1$ for a convenient timescale t_f. Thus, a full partition $A_1, \ldots, A_n$ of the state space E is called *metastable* if

$$\sum_{k=1}^{n} \mathbb{P}_\mu(X_{t_f} \in A_k \mid X_0 \in A_k) \approx n. \tag{2.1}$$

Then each of the sets A_k is almost invariant with respect to timescale t_f; the probability to stay in one of the partition sets being started there is almost 1, while the probability to change between any two different partition sets is almost 0. Such a partition is also called a *metastable decomposition*.

Obviously, being "close to 1" or "close to n" are rather vague statements. However, that lack of concreteness will be eliminated later, since we will only be interested in the "best" metastable decomposition. That means that we want to obtain a decomposition where the probability to stay inside of each metastable set is as close as possible to 1, resulting in the sum (2.1) being as close as possible to n. Likewise, the choice of the timescale t_f is not specified in general and depends on the particular system in consideration. Hence, the only parameter in (2.1) that has to be determined is the number n of subsets we are looking for.

Metastability in Molecular Systems

Metastability is a very important concept for stochastic processes corresponding to molecular systems. Such processes describe the movement of atoms or molecules in space and have the characteristic behaviour to oscillate or fluctuate around equilibrium positions on the smallest time scales. In contrast to these fast oscillations, the process often remains inside of a certain region, called *conformation*, for a long time before switching to another region. Since transitions between conformations are relatively rare events, they can be identified as metastable sets if we choose a convenient timescale. Such a behaviour is depicted in figure 2.1 on the example of the dihedral angle of a molecule, taken from Weber[53]. The dihedral angle of the presented molecule can take values between $+45°$ and $-45°$. There are two regions, highlighted red and blue, where the process stays for a rather long time and oscillates **inside**, while transition between these regions happen more infrequent. Accordingly, these two conformations can be identified as metastable sets.

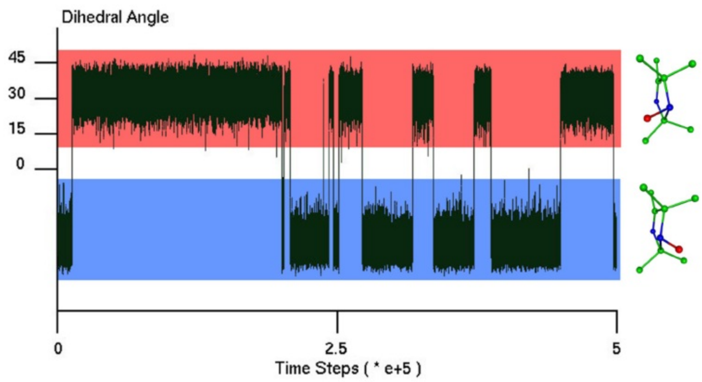

Figure 2.1: Two conformations of the dihedral angle of a molecule.

As transitions between metastable sets are rare events, long-time simulations of a process are required in order to observe conformational changes. However, long-time simulations of such large systems are not feasible in reasonable time even with the best computers nowaday, see Anton[44] or its successor Anton2[45], two supercomputers which have been designed with the special purpose to perform extensive molecular dynamics simulations.

Hence, in order to be able to execute long-time simulations of a molecular system, a reduction of complexity is needed. This can be achieved by a clustering of the state space via a Galerkin projection as described in section 1.3. Different states are clustered appropriately such that a process on a smaller state space is obtained.

This point of view also motivates the following terminology. A state in the original state space is called a *micro state*, as it is a state considered on the microscopic or atomistic level. In order to obtain a smaller state space, micro states are grouped together and such a cluster is called a *macro state*, since we are now considering the process on a macroscopic level. Consequently, we lose some information and cannot distinguish between the micro states in the reduced model anymore.

For instance, coming back to figure 2.1. The dihedral angle of the presented molecule can take infinitely many values between $+45°$ and $-45°$, representing the micro states. We can decompose the state space into two macro states, depicted red and blue. In doing so, we achieved a significant reduction of dimension from infinitely many micro states to two macro states. However, when working on this smaller state space, we cannot distinguish between the angular values from $+10°$ and $+45°$ anymore. From the macroscopic point of view, they are "the same".

Clustering into Metastable Sets

The question how to cluster a process such that the long time-scales are maintained can be answered with the following intuitive approach: As the long-term behaviour of a process is mainly determined by rare conformational changes, we choose the metastable sets as clustering sets. More clearly, a new process is created such that each macro state is **identified** to one of the metastable sets. In order to correctly represent the original process, the transition probabilities between the macro states should correspond to the transition rates between the metastable sets.

As metastability is determined on long timescales, the projected process maintains the long-time behaviour of the original process, but forgets about short-time transitions, i.e. transitions inside of a conformation. Since there is not one unique metastable decomposition of the state space, we need to find a decomposition which is in some sense "the best". In the next sections, we will clarify how to find such a decomposition.

Most importantly, the clustered process has the desired property of a reduced complexity since the model acts on a smaller state space. Therefore, the computation effort for long-time simulations is significantly decreased. Furthermore, we get a better overview of the system, since it is easier to consider a process on a few states in comparison to a process on a very large or even continuous state space. However, it has to be guaranteed that the clustered process represents the **correct** long-term behaviour of the process. That will be ensured in section 2.3, where we present a suitable projection under which the projection error vanishes.

2.2 Spectral Approach

In this section, we demonstrate the strong relation of the metastability of a Markov process to the spectrum of the associated transfer operator. More precisely, the existence of metastable sets implies the existence of dominant eigenvalues of the transfer operator and vice versa. The idea to detect metastable sets via dominant eigenvalues has been first proposed by Dellnitz and Junge[12] and transferred to molecular dynamics by Schütte et al[39, 40].

Existence of Dominant Eigenvalues

We consider the transfer operator $\mathcal{P} := \mathcal{P}(\tau)$ of a Markov process for some fixed lag-time τ in the Hilbert space $L^2(\mu)$. We are interested in *dominant eigenvalues* of $\mathcal{P}$, that is large eigenvalues which are close to 1 and separated from the rest of the spectrum. The *discrete spectrum* $\sigma_{\text{discr}}(\mathcal{P})$ is the set consisting of all eigenvalues $\lambda \in \sigma(\mathcal{P})$ that are isolated and of finite multiplicity. The *essential spectral radius* $r_{\text{ess}}(\mathcal{P})$ is defined as

$$r_{\text{ess}}(\mathcal{P}) = \inf\{r \geq 0 \mid \lambda \in \sigma(\mathcal{P}) \text{ with } |\lambda| > r \text{ implies } \lambda \in \sigma_{\text{discr}}(\mathcal{P})\}.$$

The existence of dominant eigenvalues requires that the continuous part of the spectrum is bounded away from the dominant elements of the discrete spectrum. To ensure that the process actually possesses metastable sets, we need to pose some conditions on the spectrum of the transfer operator:

C1 The essential spectral radius of $\mathcal{P}$ is less than one, i.e. $r_{\text{ess}} < 1$.

C2 The eigenvalue $\lambda = 1$ of $\mathcal{P}$ is simple and dominant, i.e.

$$\eta \in \sigma(\mathcal{P}) \text{ with } |\eta| = 1 \text{ implies } \eta = 1.$$

We will not go into further details for which processes the two above conditions are fulfilled; some criteria can be found in Huisinga[21, chapter 4]. Since we are interested in a metastable behaviour, we assume that the processes under investigation satisfy these conditions. We need condition **C1** to ensure that the continuous part of the spectrum is bounded away from the discrete eigenvalues. Otherwise they would not be dominant anymore and the process would rather be rapidly mixing than having any metastable sets. Condition **C2** however is important because the state space of a transfer operator with more than one eigenvalue of absolute value 1 can be decomposed into invariant sets, i.e. subsets which cannot be left. However, such a case is not interesting for us. Instead, we want to know more about **almost** invariant sets and their critical transition regions.

The transfer operator $\mathcal{P} : L^2(\mu) \to L^2(\mu)$ of a reversible process satisfying the properties **C1** and **C2** is self-adjoint by theorem 1.12 and has a spectrum of the form

$$\sigma(\mathcal{P}) \subset [a, b] \cup \{\lambda_n\} \cup \cdots \cup \{\lambda_2\} \cup \{1\}$$

with $-1 < a \leq b < \lambda_n \leq \cdots < \lambda_1 = 1$ and isolated, not necessarily simple eigenvalues of finite multiplicity that are counted according to multiplicity.

Relation of Dominant Spectrum to Metastability

In order to assess the quality of an arbitrary decomposition, we present upper and lower bounds for the metastability of the decomposition in terms of dominant eigenvalues and eigenfunctions of the transfer operator. We will denote by *metastability of a decomposition* the sum of the metastability of its subsets.

Theorem 2.1. (Huisinga and Schmidt[22, Theorem 2.4 and Theorem 2.5]) *Let $\mathcal{P}$ be the transfer operator of a reversible process $(X_t)_{t\in\mathbb{T}}$ satisfying* **C1** *and* **C2**. *Let $\lambda_1, \dots, \lambda_n$ denote its isolated eigenvalues and $\mathcal{X}_1, \dots, \mathcal{X}_n$ the corresponding eigenfunctions, normalized to $\|\mathcal{X}_i\|_2 = 1$. The metastability of an arbitrary decomposition into sets $A_1, \dots, A_n$ of the state space E can be bounded by*

$$\sum_{i=1}^{n} \rho_i \lambda_i + c \leq \sum_{i=1}^{n} \mathbb{P}_\mu(X_1 \in A_i \mid X_0 \in A_i) \leq \sum_{i=1}^{n} \lambda_i,$$

where $\rho_j = \|Q\mathcal{X}_j\|^2_{L^2(\mu)} \in [0,1]$ and $c = a(1-\rho_1)\cdots(1-\rho_n)$ and Q denotes the orthogonal projection of $L^2(\mu)$ onto $\{\mathbb{1}_{A_1}, \dots, \mathbb{1}_{A_n}\}$.

Theorem 2.1 reveals the connection between metastable sets and the dominant spectrum of the transfer operator. It allows us to evaluate the quality of a decomposition by comparing the lower and the upper bound of metastability. The upper bound shows that eigenvalues far away from 1 worsen the metastability of a decomposition, i.e. high eigenvalues are **necessary** for a high metastability. The lower bound is close to the upper bound if the dominant eigenfunctions $\mathcal{X}_1, \dots, \mathcal{X}_n$ are almost constant on the subsets $A_1, \dots, A_n$, implying $\rho_j \approx 1$ and $c \approx 0$, i.e. such eigenfunctions **guarantee** a high metastability. Moreover, Huisinga and Schmidt[22] show that the lower and upper bounds from theorem 2.1 are sharp and asymptotically exact. That provokes the question if there exists an **optimal** decomposition with the highest possible metastability. By all means, this theorem indicates that the number of metastable sets should be determined by the number of dominant eigenvalues.

Figure 2.2 provides a good overview of the relation between the eigenfunctions of the transfer operator and the metastable sets of the corresponding process. We consider a finite random transition matrix P consisting of four highly metastable regions with small transition probabilities between them. We clearly identify four dominant eigenvalues $\lambda_1, \dots, \lambda_4$, which are well separated from the rest of the spectrum, indicating the number of metastabilities. The corresponding eigenvectors $X_1, \dots, X_4$ are almost constant on the metastable sets.

This relation can be explained as follows. A process consisting of n invariant sets $\{A_1, \dots, A_n\}$ has the n-fold eigenvalue 1 and the corresponding eigenvectors $\mathbb{1}_{A_i}$ are constant on the invariant sets. A metastable process consists of almost invariant sets and can be interpreted as the perturbation of a process with invariant sets, by introducing small transition probabilities between the invariant sets. Accordingly, the eigenvalues and eigenvectors are perturbed. This results in one eigenvalue 1 and $n-1$ eigenvalues close to 1, corresponding to eigenvectors that are almost constant on the almost invariant sets. A detailed perturbation analysis can be found in Deuflhard et al[13].

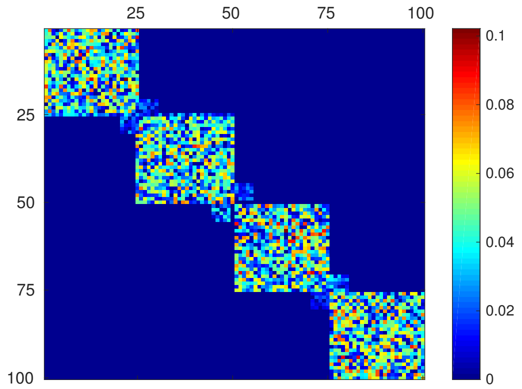

(a) Transition matrix P on 100 states with 4 visible metastable sets

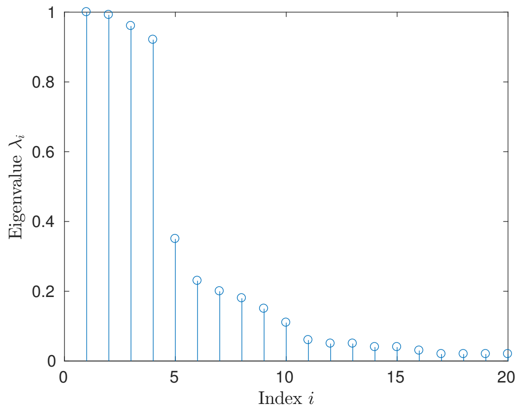

(b) Spectrum of P with 4 dominant eigenvalues

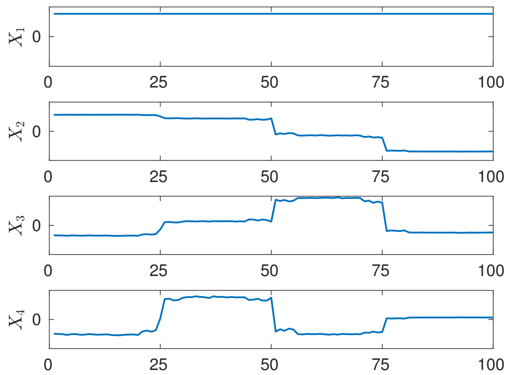

(c) Dominant eigenvectors of P indicating the metastable sets

Figure 2.2: Relation of the transition matrix to its spectrum with regard to metastability

There exist algorithms[13] to identify the metastable sets of a Markov chain by exploiting the sign structure of the dominant eigenvectors of the transition matrix. That is one possible method to cluster a process with respect to metastability, though it bears some disadvantages. In particular, such a full-partition decomposition of the state space does not take into consideration the existence of transition regions and can lead to an iteration error.

This section has been presented mainly with the aim to emphasize the strong relation of the spectrum of the transfer operator to the metastability of the system. However, this approach does **not** represent the state of the art. In the next section, we deduce an enhanced method, as well based on the dominant spectrum, though resulting in a **soft** clustering instead of a full partition decomposition.

2.3 Fuzzy Clustering

The above considerations yield a metastable full decomposition of the state space, assigning each state to **exactly** one of the partition sets. Indeed, there exist more accurate solutions, considering the fact that states in transition regions are adjacent to several conformations and therefore cannot be uniquely assigned to one of them. We introduce a more general concept, allowing some "overlap" between the conformations.

Set-based vs. Function-based Approach

The intuitive approach to decompose the state space of a process is to determine a certain number of metastable sets which form a full partition, such that each micro state belongs to exactly one of them. The problem with that approach is that likewise each state in a transition region has to be assigned to one of these partition sets. Though why would we assign a state in a transition region to one particular adjacent conformation and not to another one? Such a strict assignment is obviously not an accurate description of the actual behaviour of the process.

Therefore, this *set-based* clustering method has been replaced by a *function-based* method, which means that the states are assigned with certain "degrees" to the conformations. This approach is justified by the existence of transition regions. A state inside of a transition region, for instance around a local energy maximum, can enter into different adjacent metastable sets with similar probabilities. Therefore, instead of assigning it to a single conformation, we define that it should belong to each of these adjacent conformations with a certain degree. In that sense, the conformations may be "overlapping".

Membership Functions

We consider the transfer operator $\mathcal{P}$ of a Markov process having n dominant eigenvalues. Consequently, we aim to create a Markov State Model on n states, representing the metastable sets of the process. We follow the approach of Weber[52] to define macro states as *overlapping partial densities*. They can be identified by membership functions assigning degrees of membership to the micro states.

Definition 2.2. (Membership Function)
The functions $\chi_1, \ldots, \chi_n : E \to [0, 1]$ are called *membership functions* if they fulfill

- $\chi_j(x) \geq 0\ \forall i \in E$ and $\forall j \in \{1, \ldots, n\}$ (positivity),
- $\sum_{j=1}^{n} \chi_j(x) = 1\ \forall x \in E$ (partition of unity).

The value $\chi_j(x)$ is the *degree of membership* of micro state x to macro state j. In the following, the membership function χ_j will also be denoted as the conformation j it represents.

The example of a full-partition discretization corresponds to the choice of characteristic functions $\{\mathbb{1}_{A_1}, \ldots, \mathbb{1}_{A_n}\}$ as membership functions. Each micro state is uniquely assigned to one of the partition sets, without any overlap. Therefore, such a clustering is called *crisp* or *hard*, whereas the general, possibly overlapping, membership functions result in a *fuzzy* or *soft* clustering. As there are many possible membership functions, we need to find a choice that yields a reasonable metastable decomposition.

Usually they are chosen to be **close** to a characteristic function, also called *almost characteristic function*, as depicted in figure 2.3. Such a choice is plausible, since it puts the emphasis of a conformation on a certain region by assigning a high degree of membership, though likewise includes the adjacent transition regions by a low degree of membership. Thus, they fulfill the following two desired conditions:

- There should be a **soft** assignment inside of a transition region, in order to respect the ambiguous membership of transition states.
- The clustering should be **crisp** enough to distinguish the conformations.

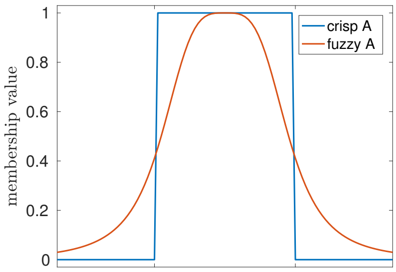

Figure 2.3: The crisp set A is represented by a characteristic function and approximated by an "almost characteristic function".

These requirements are clarified in figure 2.4 at the recurring example of a double-well potential, i.e. a system consisting of two conformations with one transition region between them. A crisp clustering does not consider the transition region (a), while a "very fuzzy" choice of membership functions does not represent the conformations (c). The degrees of membership are no actual probabilities, yet they can be interpreted as such. Consider for instance the energy maximum of the double well potential. This transition state tends with the same probability to the left and to the right well. Therefore it seems plausible to assign it with the same degree of membership to both conformations. On the other hand, a state in the middle of a well cannot immediately jump into the other well, therefore this transition probability is 0 and the state can be assigned with degree of membership 1 to the conformation corresponding to its well. That is fulfilled by the almost characteristic functions in figure 2.4 (b).

This illustrative justification for the choice of almost characteristic functions as membership functions can be combined with theorem 2.1, stating that the metastability of a decomposition $A_1, \ldots, A_n$ is high if the eigenfunctions $\mathcal{X}_1, \ldots, \mathcal{X}_n$ are well approximated by characteristic functions $\mathbb{1}_{A_1}, \ldots, \mathbb{1}_{A_n}$. This high metastability is preserved by choosing a linear combination of the eigenfunctions. Consequently, we aim to find membership functions $\chi_1, \ldots, \chi_n$ in $\operatorname{span}\{\mathcal{X}_1, \ldots, \mathcal{X}_n\}$ with

$$\chi_i \approx \mathbb{1}_{A_i}.$$

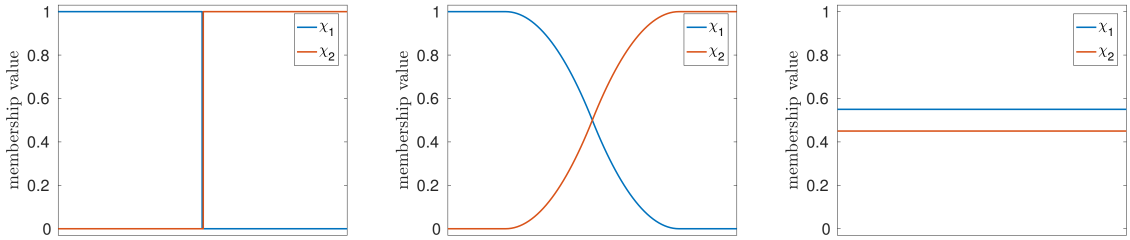

(a) Characteristic functions resulting in a hard clustering.
(b) Almost characteristic functions resulting in a soft clustering.
(c) Very soft and useless membership functions.

Figure 2.4: Possible membership functions χ: From hard to fuzzy clustering.

Perron Cluster Analysis

The term *Perron Cluster Analysis* denotes the objective of clustering a Markov process into metastable sets using the *Perron eigenvalues* and *Perron eigenfunctions*, being eigenvalues close to 1 and their associated eigenfunctions. Perron Cluster Analysis respectively its algorithmic implementation PCCA ("Perron Cluster Cluster Analysis") has been developed by Deuflhard et al[13], employing the sign structure of the dominant eigenvalues of the transition matrix. This approach has been improved by Deuflhard and Weber[14] who transformed the system of eigenvectors into a system of membership functions resulting in a fuzzy clustering of the state space; their algorithm is called PCCA+ ("Robust Perron Cluster Analysis"). The formulation is even valid for continuous processes, see Weber[53].

Let $\mathcal{P} := \mathcal{P}(\tau)$ on $L^2(\mu)$ be the transfer operator describing a **reversible** process, i.e. $\mathcal{P}$ is μ-self-adjoint by theorem 1.12. We consider the set of dominant eigenvalues $\{\lambda_1, \dots, \lambda_n\}$ with the corresponding set of normalized eigenfunctions $\mathcal{X} = \{\mathcal{X}_1, \dots, \mathcal{X}_n\}$. They fulfill the eigenvalue equation $\mathcal{P}\mathcal{X} = \mathcal{X}\Lambda$ of the transfer operator $\mathcal{P}$, with $\Lambda = \mathrm{diag}(\lambda_1, \dots, \lambda_n)$. The set of membership functions $\chi = \{\chi_1, \dots, \chi_n\}$ can be built as a linear combination $\mathcal{X}A$ of the dominant eigenfunctions, that is

$$\chi_j(x) = \sum_{i=1}^{n} A_{ij}\mathcal{X}_i(x), \ j = 1, \dots, n, \tag{2.2}$$

where $A = \{A_{ij}\}_{i,j=1,\dots,n} \in \mathbb{R}^{n\times n}$ is a regular matrix. It has to be chosen in such a way that the resulting membership functions χ fulfill the positivity and partition of unity constraints. As there are infinitely many such transformations A of the eigenfunctions, we have to determine one that satisfies some optimality condition. The algorithm PCCA+ computes the transformation matrix A as the solution of a **convex** maximization problem, see Weber[52]. With the resulting membership functions, the Galerkin projection is given by

$$P_c(\tau) = G(\mathcal{P}(\tau)) = (\langle \chi, \chi \rangle_\mu)^{-1}(\langle \chi, \mathcal{P}(\tau)\chi \rangle_\mu). \tag{2.3}$$

The following theorem shows that for any such linear combination of the eigenfunctions $\chi = \mathcal{X}A$, the discretization error of the projection vanishes. Hence, diagram 1.2 commutes, implying that propagating and projecting of a transfer operator are commutative actions. In particular, such membership functions preserve the Markov property.

Theorem 2.3. (Weber [53, Theorem 2])
Let $\mathcal{P} := \mathcal{P}(\tau)$ be a μ-self-adjoint transfer operator with a set $\mathcal{X} = \{\mathcal{X}_1, \ldots, \mathcal{X}_n\}$ of normalized eigenfunctions s.t. $\mathcal{P}\mathcal{X} = \mathcal{X}\Lambda$, where $\Lambda = \mathrm{diag}(\lambda_1, \ldots, \lambda_n)$ is the eigenvalue matrix. Let $\chi = \mathcal{X}A$ be a set of functions that is a linear combination of the eigenfunctions $\mathcal{X}$ with a regular $n \times n$-transformation matrix A as defined in (2.2)*. Then the iteration error for the Galerkin discretization $P_c = G(\mathcal{P})$ vanishes.*

Proof. The Galerkin projection of the transfer operator $\mathcal{P}$ is computed by

$$\begin{aligned} G(\mathcal{P}) &\overset{(2.3)}{=} (\langle \chi, \chi \rangle_\mu)^{-1} (\langle \chi, \mathcal{P}\chi \rangle_\mu) \\ &\overset{(2.2)}{=} (A^T \langle \mathcal{X}, \mathcal{X} \rangle_\mu A)^{-1} (A^T \langle \mathcal{X}, \mathcal{P}\mathcal{X} \rangle_\mu A) \\ &= (A^T \langle \mathcal{X}, \mathcal{X} \rangle_\mu A)^{-1} (A^T \langle \mathcal{X}, \mathcal{X} \rangle_\mu \Lambda A) \\ &= (A^T A)^{-1} (A^T \Lambda A) \\ &= A^{-1} \Lambda A. \end{aligned}$$

The last two lines are obtained by inserting the eigenvalue problem $\mathcal{P}\mathcal{X} = \mathcal{X}\Lambda$ and employing the μ-orthogonality of the eigenfunctions by theorem 1.11, and therefore $\langle \mathcal{X}, \mathcal{X} \rangle_\mu = \mathcal{I}$, being the identity operator. In particular, after k time-steps we have

$$(G(\mathcal{P}))^k = (A^{-1} \Lambda A)^k = A^{-1} \Lambda^k A = G(\mathcal{P}^k). \qquad \square$$

In this proof, the reversibility of the process is essential. Otherwise the transfer operator is not self-adjoint and possibly possesses complex eigenvalues, leading to complex-valued eigenfunctions, which cannot be transformed into meaningful membership functions. In order to tackle non-reversible processes as well, an enhanced method is presented in section 2.4.

Even though the algorithm of PCCA+ is valid for continuous processes defined by a transfer operator $\mathcal{P}$, for real applications a discretization of $\mathcal{P}$ to a matrix P is necessary:

$$\mathcal{P} \to P \to P_c.$$

One possible approach for that intermediate step are direct sampling methods, counting transitions between subsets. However, since long-time simulations are required in order to obtain valuable informations about transitions between metastable sets, they are not the best choice. Another option are adaptive sampling methods, for instance Voronoi tesselation, see Weber[53]. Having a discrete matrix P, it is easy to compute the eigenvalues and eigenvectors in order to apply PCCA+ and obtain a clustered matrix P_c.

Objective Function: Crispness of Membership Functions

Each macro state yields a statistical weight

$$w_j = \langle \chi_j, \mathbb{1} \rangle_\mu = \int_E \chi_j(x)\mu(\mathrm{d}x).$$

The statistical weight vector $w = (w_1, \ldots, w_n)$ coincides with the left eigenvector of the matrix representation $P_c = S^{-1}T$, see theorem 1.19. The diagonal matrix $D = \mathrm{diag}(w_1, \ldots, w_n)$ consists of the statistical weights of the membership functions. Then the matrices S and T can be expressed as

$$\begin{aligned} T &= D^{-1}\langle \chi, \mathcal{P}\chi \rangle_\mu = D^{-1}A^T \Lambda A \quad \text{and} \\ S &= D^{-1}\langle \chi, \chi \rangle_\mu = D^{-1}A^T A. \end{aligned} \tag{2.4}$$

Different objective functions for PCCA+ are possible, some are proposed in Weber[52, chapter 3.4]. Originally, one objective was to maximize the metastability of the conformations by maximizing trace(T). In the context of stochastic matrices, a high trace corresponds to a high determinant, since trace(T) is bounded by above from n and det(T) by 1. This upper bound is achieved only for the identity matrix, thus for a “strong diagonal”. Increasing the trace towards n is equivalent to increasing the determinant towards 1. Since the trace is not multiplicative, we resort to the determinant to calculate the following relation:

$$\begin{aligned} \det(T) &= \det(S)\det(A^{-1}\Lambda A) \\ &= \det(S)\det(\Lambda) \\ &= \det(S)\Pi_{i=1}^n \lambda_i. \end{aligned}$$

In order to obtain a high metastability, both factors on the right side need to be high. The term $\det(\Lambda)$ is high if the dominant eigenvalues λ_i are as close as possible to 1, whereas $\det(S)$ is maximized if the membership functions $\chi = \mathcal{X}A$ are as **crisp** as possible. That means that they are as orthogonal as possible, having only few overlap. Since S is a stochastic matrix as well, maximizing its determinant is equivalent to maximizing its trace.

Thus, maximizing trace(S) is a plausible objective, since it provides a clustering with high metastability, while the metastable sets are well distinguishable because of the crispness. This choice was proposed by Röblitz[33]. Moreover, trace is a **convex** function, which is a necessary criterion for the objective function of PCCA+:

$$\max_{A \in \mathbb{R}^{n \times n}} \mathrm{trace}(S) \quad \text{such that } \chi = \mathcal{X}A \geq 0 \text{ and } \sum_j \chi_{ij} = 1. \tag{2.5}$$

One example for the presented procedure is shown in figure 2.5, continuing the example from section 2.2. The optimal membership functions $\chi = XA$ are computed as a linear combination of the dominant eigenvectors $X_1, \ldots, X_4$ by PCCA+ and have only few overlap, according to the objective (2.5). The Galerkin projection yields the low-dimensional matrix representation P_c revealing the four strongly metastable subsets.

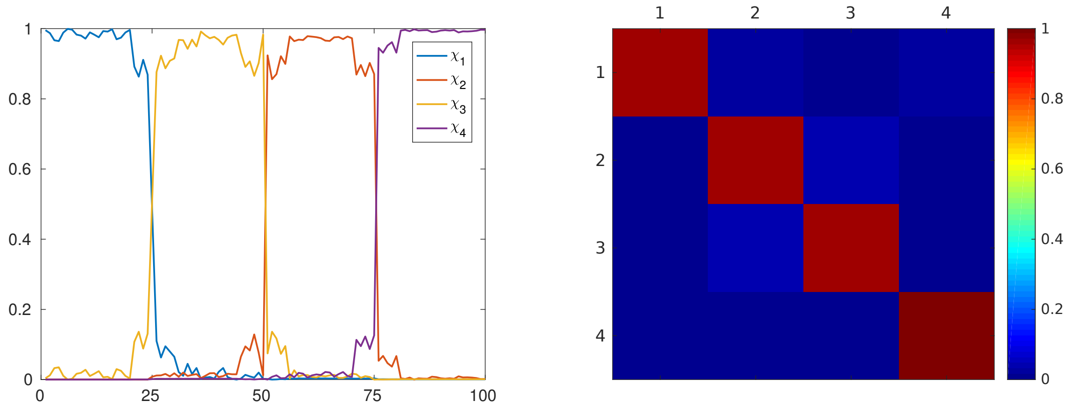

(a) Membership functions χ.

(b) Matrix P_c with a reduced dimension.

Figure 2.5: Clustering of a metastable process by fuzzy membership functions (PCCA+).

Matrix Representation of Projection

For the later investigations, we are interested in analyzing the matrix representation $P_c = S^{-1}T$. The entries of S are defined by the scalar products of the membership functions, meaning that the *crispness* of a clustering can be measured by the matrix S. Nonoverlapping membership functions yield a matrix S equal to the unit matrix, while overlapping membership functions result in a matrix with non-zero outer diagonal elements. The higher the outer diagonal elements, the higher the overlap. Therefore the diagonal of S can be seen as a "measure of crispness" of the $\chi_1, \ldots, \chi_n$. We recall that a full-partition decomposition yields a matrix S being equal to the identity matrix, justified by the orthogonality of the characteristic functions. With the motivation to choose almost characteristic functions as membership functions, the χ_i are still close to being orthogonal and therefore, S should be close to the identity matrix.

The dynamical behaviour of $\mathcal{P}$ is encoded in the coupling matrix T, while S merely describes the overlap of the membership functions. If S is close to the identity matrix, then the dynamics of the projected process is almost completely determined by T. In contrast, if S deviates from identity, then it may influence the dynamics rather strongly. The actual meaning of this contribution of the overlap to the dynamics will be emphasized in chapter 3.

The fuzzy clustering method presented in this section unifies many significant advantages. In contrast to crisp decompositions, the soft approach takes into consideration the ambiguous membership of states in transition regions. The choice of overlapping membership functions ensures that the projection error vanishes, which is crucial for a correct mapping. Most importantly, PCCA+ maximizes the metastability of the conformations and thereby provides the "best" clustering. However, this result is restricted to reversible processes, since orthogonal and real eigenfunctions were required for theorem 2.3.

2.4 Schur Decomposition

All previous projections of processes onto their metastable sets were based on the assumption of reversibility. Unfortunately, many real-world processes are not reversible. In that case, the transfer operator is not self-adjoint and might have complex eigenvalues and eigenfunctions, which cannot be transformed into real membership functions. This problem can be circumvented by considering a real Schur decomposition instead of the spectral decomposition. This approach yields an invariant subspace of real Schur vectors spanning the same subspace as the corresponding eigenvectors[20] and fulfilling the required conditions for the use of PCCA+. Thus, we employ the same method as before, though replace eigenvectors by Schur vectors. Beyond enabling us to analyze non-reversible processes, this new approach has some more advantages, like allowing us to identify dominant cycles.

NESS processes

A Markov process is called *nonequilibrium steady state* (NESS) process if it is nonreversible, but still has a steady state, given by an invariant measure π, such that the process is ergodic with respect to π. As a NESS process is nonreversible, there are regions where the detailed balance equation is not fulfilled, i.e. there is an effective probability flow $p(\tau, A, B) - p(\tau, B, A) \neq 0$ between some subsets $A, B \subset E$ of the state space.

In the following, we consider an ergodic Markov chain on the finite state space $E = \{1, \ldots, N\}$ given by the transition matrix P. By irreducibility, the process possesses a unique stationary distribution π being positive everywhere. Then π is the normalized eigenvector of P associated to the unique eigenvalue $\lambda_1 = 1$.

Definition 2.4. (Flow Matrix)
The probability flow associated to a Markov chain is given by the flow matrix

$$F = DP,$$

where P is the transition matrix of the process and D the diagonal matrix $D = \mathrm{diag}(\pi_1, \ldots, \pi_N)$ with the entries of the stationary distribution π.

The steady state probability flow from state i to j is given by $F_{ij} = \pi_i P_{ij}$. If the process is reversible, the flow matrix F is symmetric due to detailed balance. For a NESS process, F is not symmetric since there are states $i, j \in E$ with $F_{ij} \neq F_{ji}$.

Schur Decomposition

We have the same objective as in the previous section: given a Markov process acting on a large state space E, a projection onto a smaller state space $\{1, \ldots, n\}$ is aimed at, such that each cluster represents one metastable set of the process. For this purpose, we introduce a matrix decomposition generalizing the spectral decomposition.

Definition 2.5. (Schur Decomposition)
Let $P \in \mathbb{R}^{N \times N}$ be a transition matrix. Then it can be written as

$$X^{-1}PX = \Lambda, \tag{2.6}$$

where X is a unitary matrix and Λ is an upper triangular matrix, having $\lambda_1, \ldots, \lambda_N$ as diagonal entries, which is called a *Schur decomposition* of P. If $X = [v_1 \mid \cdots \mid v_N]$ is a column partitioning of X, then the v_i are referred to as *Schur vectors.*

The existence of such a matrix X is shown in Golub and van Loan[20, theorem 7.1.3]. Since Λ is similar to P, both matrices have the same eigenvalues. Since Λ is triangular, they correspond to the diagonal entries $\lambda_1, \ldots, \lambda_N$ of Λ. The Schur vectors v_k satisfy

$$Pv_k = \lambda_k v_k + \sum_{i=1}^{k-1} n_{ik} v_i, \quad k = 1, \ldots, N,$$

and therefore span an invariant subspace given by

$$S_k = \operatorname{span}\{v_1, \ldots, v_k\}.$$

Moreover, if we choose a matrix $X_k = [v_1 \mid \cdots \mid v_k]$, then $\sigma(X_k^{-1}PX_k) = \{\lambda_1, \ldots, \lambda_k\}$. The eigenvalues λ_i in (2.6) can be arbitrarily ordered by an appropriate choice of X. Thus, each subset of k eigenvalues induces at least one k-dimensional invariant subspace.

For our purpose, decomposition (2.6) is not sufficient, since it can include complex Schur vectors. As P is a real matrix, its non-real eigenvalues come in complex conjugate pairs[20]. This fact can be utilized to build a *real Schur decomposition*, where both X and Λ are real matrices. This alternative decomposition does not yield a triangular matrix, but only a *quasi-triangular* one, allowing 2×2-blocks on its diagonal.

Theorem 2.6. (Real Schur Decomposition)
If $P \in \mathbb{R}^{N \times N}$, then there exists an orthogonal matrix $X \in \mathbb{R}^{N \times N}$ such that

$$X^{-1}PX = \Lambda_s,$$

where Λ_s is block-triangular with 1×1 and 2×2-blocks on its diagonal. The 1×1-blocks contain the real eigenvalues of P and the eigenvalues of the 2×2-blocks are the complex eigenvalues of P.

A proof can be found in Golub and van Loan[20, theorem 7.4.1]. Each real matrix can be decomposed into such a quasi-triangular matrix. Thus, the real Schur decomposition can be considered as an "eigenvalue-revealing" decomposition; the real and the imaginary part of the complex eigenvalues are easily obtained from the 2×2-blocks.

Block-diagonal Structure

We want to make use of the real Schur decomposition to analyze transition matrices. Considering the quasi-triangular matrix Λ_s, we can not only find out informations about the eigenvalues of P, but also on the reversibility of the process. A case study is presented in Weber[54] and shortly summarized in the following.

By definition, the reversibility of a process is determined by the flow matrix $F = DP$. According to detailed balance, a process is reversible if and only if this matrix is symmetric. However, nonreversibility of P can as well be identified by its real Schur decomposition Λ_s, having a block-diagonal shape. The meaning of an 1×1-block as an eigenvalue is clear, so we simply analyze the shape of such an 2×2-block and its influence on the reversibility and the spectrum of P. Assume we are given the Schur decomposition

$$\Lambda_s = \begin{pmatrix} 1 & 0 & 0 \\ 0 & \lambda_2 & \epsilon \\ 0 & -\delta & \lambda_3 \end{pmatrix}$$

with non-negative parameters $\epsilon, \delta \geq 0$. We examine the properties of this matrix by inserting different values for ϵ and δ in the 2×2-block.

Reversible If $\epsilon = \delta = 0$ and furthermore $\lambda_2 \neq \lambda_3$, then Λ_s is a diagonal matrix and P is reversible. In this case, the Schur decomposition is identical to the spectral decomposition and in particular, the Schur vectors correspond to the eigenvectors.

Reversibility of P is equivalent to the symmetry of Λ_s.

Nonreversible with real eigenvalues Adding an additional upper diagonal element $\epsilon > 0$ makes Λ_s asymmetric. The eigenvalues of P correspond to the entries $\lambda_1, \dots, \lambda_n$ on the diagonal of Λ_s. The eigenvectors of P are real, but **not π-orthogonal** anymore. In contrast to that, the Schur vectors are still π-orthogonal.

Non-reversibility of P can be seen by the fact that the Schur matrix Λ_s is not symmetric.

Nonreversible and not diagonalizable If $\lambda_2 = \lambda_3$ with $\epsilon > 0$ and $\delta = 0$, then P has an "incomplete" 2×2-block, implying that it has an eigenvalue with different geometrical and algebraic multiplicity. Therefore, P has no spectral decomposition and is **not diagonalizable**, whereas the Schur decomposition still exists.

Since P is not diagonalizable, it is non-reversible.

Nonreversible with complex eigenvalues If $\lambda_2 = \lambda_3$ and additionally $\epsilon, \gamma > 0$, then we have a "complete" 2×2-block, encoding the existence of two **complex eigenvalues**.

The complex-valued spectrum implies the non-reversibility of P. However, the Schur decomposition still yields **real** Schur vectors.

Summarized, there are several problems that can occur when dealing with the eigendecomposition of non-reversible processes. The existence of a spectral decomposition is not always given. Moreover, it can happen that the eigenvectors are not π-orthogonal or contain complex entries, which is problematic for the use of PCCA+. However, we can circumvent these issues by employing the real Schur vectors instead.

GenPCCA: Clustering in terms of Schur vectors

The aim is to cluster a given process P into metastable sets based on membership functions $\chi = XA$. However, the application of PCCA+ requires certain conditions to be fulfilled in order to yield a meaningful projection, which is in general not the case for eigenvectors of a non-reversible process. A solution replacing them by Schur vectors has been proposed by Fackeldey and Weber[16]. Their approach is a generalization of PCCA+ and therefore called Gen-PCCA ("Generalized-Perron Cluster Cluster Analysis").

Looking back to the proof of theorem 2.3, we identify two conditions implying a correct projection, i.e. a projection without discretization error. The matrix $X \in \mathbb{R}^{N\times n}$ has to span an invariant subspace by

$$PX = X\Lambda \tag{2.7}$$

for $\Lambda \in \mathbb{R}^{n\times n}$. Furthermore, the orthogonality relation

$$X^T D_\eta X = I, \tag{2.8}$$

has to be satisfied with respect to some initial distribution η.

These properties are in general not fulfilled for the spectral decomposition of a nonreversible process, as we can see from a comparison with the previous case study. For a non-reversible process, the eigenvectors can be complex or non-orthogonal. Moreover, it is not even guaranteed that P is diagonalizable. In contrast to that, a set of real Schur vectors for a stochastic matrix P can always be constructed such that it satisfies both criteria. In order to do so, the following symmetrization trick can be applied. If $\widetilde{X}$ are n Schur vectors of $\widetilde{P} = D^{0.5}PD^{-0.5}$, with $D = D_\eta$, then we get

$$\begin{aligned}
& \widetilde{P}\widetilde{X} = \widetilde{X}\Lambda_s \\
\Leftrightarrow\quad & D^{0.5}PD^{-0.5}\widetilde{X} = \widetilde{X}\Lambda_s \\
\Leftrightarrow\quad & PD^{-0.5}\widetilde{X} = D^{-0.5}\widetilde{X}\Lambda_s \\
\Leftrightarrow\quad & PX = X\Lambda_s, \text{ with } X = D^{-0.5}\widetilde{X}.
\end{aligned}$$

Since Schur vectors of a symmetric matrix are always orthogonal, the same holds for its multiplication with a diagonal matrix. Thus, we are guaranteed that X fulfills conditions (2.7) and (2.8). A further advantage in comparison to the previous section is that orthogonality can be achieved for **any** initial distribution η. However, since we assume NESS processes with a stationary distribution π, we can as usual just employ orthogonality with respect to π. By this procedure, we obtained a set of orthogonal vectors X spanning an invariant subspace and we can compute an optimal transformation matrix A by applying PCCA+. Gen-PCCA can be summarized as follows:

i) Compute a real Schur decomposition $(\widetilde{X}, \Lambda_s)$ of the symmetrized matrix $\widetilde{P} = D^{0.5}PD^{-0.5}$. Then $X = D^{-0.5}\widetilde{X}$ fulfills the conditions (2.7) and (2.8).

ii) Sort the Schur values and the 2×2-blocks by using SRSchur by Brandts[6] such that they are in a descending order of their absolute value. Pick the dominant Schur values.

iii) Determine the submatrix $X \in \mathbb{R}^{N \times n}$ of n dominant Schur vectors and apply PCCA+ in order to determine the membership functions χ.

Besides metastable sets, nonreversible processes can also contain dominant cycles. They are different dominant structures representing a cyclic behaviour of the process, as described by Kalpazidou[23].

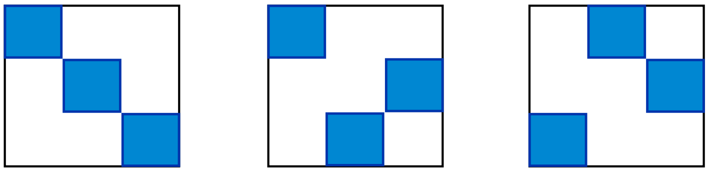

Figure 2.6: Possible structures that can be revealed by GenPCCA.

GenPCCA+ is not only able to identify metastable sets, but also cycles or mixtures of both structures, as depicted in figure 2.6. They can be detected since we consider the dominant eigenvalues and Schur blocks with respect to their absolute value. Dominant cycles are induced by complex eigenvalues $|\lambda| \approx 1$, see Djurdevac Conrad et al[15].

Conclusion

Even though the Schur decomposition is known for a long time, being described by Schur[38] in 1909, the approach to utilize it for identifying metastable sets is relatively new, proposed by Röblitz[33] in 2009 and implemented with GenPCCA[16] in 2017. There is a huge amount of scientific papers using eigenfunctions or eigenvectors to cluster a process into metastable sets. The entire framework of Markov State Models is built on the spectral analysis of the transfer operator respectively transition matrix; at the beginning in terms of hard sets, nowadays in terms of fuzzy sets. However, the employment of a Schur decomposition seems to be an appropriate enhancement of this well-known clustering method.

The main advantage is that it represents a generalization of the spectral fuzzy clustering method and thereby includes reversible as well as **non-reversible** processes. In contrast to the spectral decomposition, a real Schur decomposition **exists** for all transition matrices. The fact that the orthogonality of the Schur vectors is not restricted to the stationary measure, but can be chosen with respect to **any** initial distribution, makes this method more flexible. The detection of different **dominant structures** is a further advantage. In contrast, the disadvantages of this method are not too severe. A Schur decomposition is not unique and does not exist for a continuous transfer operator. This does not matter for most applications. Employing PCCA+ for continuous processes requires a discretization as well, even though the theory of this method is valid for continuous processes. The multitude of favorable points implies that Gen-PCCA is a very powerful tool, improving some weak points of PCCA+.

Consequently, many problems that are already solved for reversible processes can be tackled with this enhanced method in order to obtain the according results for non-reversible processes as well. For a particular optimization problem, this will be done in the next chapter.

3 Rebinding Effect in a Given Kinetics

In this chapter, we examine receptor-ligand-systems, a type of molecular systems consisting of so called receptors and ligands. These molecules interact in such a way that under certain conditions they can bind to each other and dissociate again afterwards. Such a process is originally Markovian and can be described by a transfer operator. However, by projecting this operator onto a finite-dimensional state space, the Markov property of the process may be spoiled, in a similar fashion as described in section 1.4. We explain this memory effect, the so called rebinding effect, and examine its influence on the stability of a receptor-ligand-system. We show how this effect can be measured with the tools known from the first two chapters. In particular, we present a lower bound for the rebinding effect included in a given system as the solution of an optimization problem. This estimation is deduced for reversible processes, according to Weber and Fackeldey[56], and finally extended to non-reversible processes by employing a Schur decomposition, as demonstrated in section 2.4.

3.1 Receptor-Ligand System

After introducing the basic biochemical knowledge necessary for the understanding of receptor-ligand-systems, we model a simple *receptor-ligand-system* mathematically using a differential equation. We discuss the so called rebinding effect included in this system and set it in relation to the recrossing effect known from section 1.4. As a motivation for further investigations, we explain its relevance in the application of computational drug design.

Molecular Dynamics vs Molecular Kinetics

A molecular system consists of molecules, i.e. atoms which are connected by *covalent bonds*. The motion inside of such a system can be characterized in different ways. The term *molecular dynamics* denotes the analysis of a **single** trajectory and is mainly employed in the context of simulations. It means that one initial configuration of the system is fixed and its evolution in time is observed. One example was depicted in figure 2.1, representing **one** trajectory of a stochastic system. This can give an insight about the structure of the system, like identifying possible metastabilities. However, it is not representative in the sense that a second simulation with high probability yields a different trajectory. In contrast to that, in *molecular kinetics*, an **ensemble** of trajectories is considered. Accordingly, it is formulated in terms of densities, concentrations or transition rates. However, these quantities are related to the molecular dynamics approach as they represent an average of many single realizations of a process. In this thesis, we follow the molecular kinetics approach by examining transition rate matrices.

Receptors and Ligands

The following presentation of receptor-ligand systems is based upon Lauffenburger and Linderman[27], providing a comprehensible introduction into this topic. In biochemistry, a *receptor* is a molecule, often a protein, that is usually located on the surface of a cell and can receive signals from outside the cell. A molecule that has the ability to *bind* or *associate* to a receptor is called a *ligand*. Each receptor will only bind with ligands of a particular structure, which is often referred to as the "key-lock principle". Both receptor and ligand need to have specific complementary geometric shapes that fit exactly into one another, as exemplarily depicted in figure 3.1.

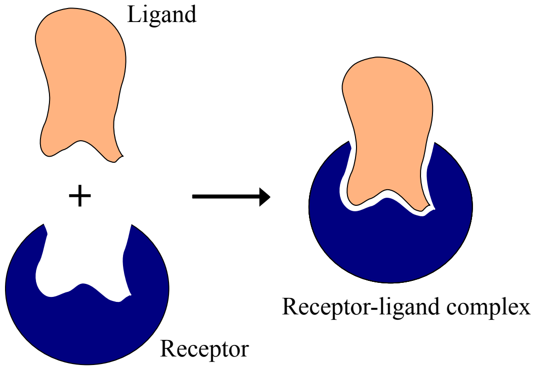

Figure 3.1: Ligand ("key") binds to a receptor ("lock"). Their shapes fit together.

Such a binding between a receptor and a ligand can *activate* ("unlock") the receptor by producing some kind of a chemical signal and thereby provoke a physiological response. For instance, that could be a conformational change in a protein, caused by a hormone binding to it. However, instead of engaging into the actual physiological consequences of a binding, we focus on the **act** of binding events.

The action of binding is typically reversible[1] through *dissociation* of the involved receptor and ligand. Ligand binding is a *chemical equilibrium* process, which means that the reaction rates of the binding and dissociating events are equal, once this equilibrium is reached. From then on, the concentrations of the reactants (ligands) and the products (complexes) are constant. It is a *dynamic equilibrium*, since reactions take place, even though no net change in the concentrations can be observed.

The binding behaviour of a simple receptor-ligand system is formalized as follows. A ligand (L) can bind to a receptor (R) and form a receptor-ligand complex (LR) which can dissociate again into its original components. This process can be represented by a reaction equation

$$\mathrm{L} + \mathrm{R} \underset{k_{\mathrm{off}}}{\overset{k_{\mathrm{on}}}{\rightleftharpoons}} \mathrm{LR}. \tag{3.1}$$

Being a process in chemical equilibrium, the law of mass action states that the ratio between the concentration of reactants and products is constant. The corresponding *dissociation*

[1]We remark that in this context, *reversible* means that a ligand can bind and unbind to a receptor, i.e. the reaction can run forward and backward, in contrast to the mathematical "reversible", meaning that a process in equilibrium behaves **equally** when running backwards in time.

constant k_d is given by

$$k_d = \frac{k_{\text{off}}}{k_{\text{on}}} = \frac{[\text{L}] \cdot [\text{R}]}{[\text{LR}]},$$

where [L] represents the concentration of unbound ligands, [R] the concentration of unoccupied receptors and [LR] the concentration of receptor-ligand complexes, respectively. This constant is used to describe the *binding affinity* between a ligand and a receptor, that is how strongly the ligand can bind to his particular receptor. If the dissociation constant is small, then there are relatively many complexes in comparison to unbound molecules, and for this reason, the binding affinity between the ligand and the receptor is high. The *association constant* k_a is the inverse of the dissociation constant

$$k_a = \frac{k_{\text{on}}}{k_{\text{off}}} = \frac{[\text{LR}]}{[\text{L}] \cdot [\text{R}]}.$$

There are different factors which can influence the binding affinity of a process. It depends on the nature of the constituent molecules, like their shape, size and possible charge. The binding affinity of a particular ligand-protein interaction can also significantly change with solution conditions, e.g. temperature, pH or salt concentration. For instance, a higher temperature leads to a faster movement of the molecules and therefore increases the probability of binding events. In general, high-affinity binding results in a higher degree of occupancy of the receptors than it is the case for low-affinity binding; the residence time does not correlate.

Mathematical Model of Receptor-Ligand-System

Starting from the reaction equation (3.1), we claim that a ligand can be found in two different macro states: “unbound” (L) or “bound” (LR). Then the probabilities of the ligand to be in one of these states are described by the probability vector $x^T = \frac{1}{s}([\text{L}], [\text{LR}])$, where $s = [\text{L}] + [\text{LR}] = \text{const.}$ is the normalization constant. This leads to an ordinary differential equation

$$\dot{x}^T = x^T Q_c.$$

The matrix Q_c consists of the rates of reaction,

$$Q_c = \begin{pmatrix} -k_a[R] & k_a[R] \\ k_d & -k_d \end{pmatrix}, \tag{3.2}$$

where k_a and k_d are the association and dissociation constants. It corresponds to the transition rate matrix of a Markov chain, that means it describes a **memoryless** process. The two possible macro states for a ligand-binding-system consisting of one receptor and one ligand are depicted in figure 3.2. We notice that the spatial arrangement of the receptor and the ligand in the unbound state is not included in the above model. Therefore, we cannot distinguish if, at a given time, the receptor and the ligand are close to each other or not.

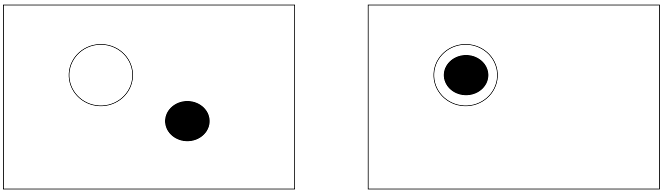

(a) "unbound" (b) "bound"

Figure 3.2: Two possible macro states of a ligand-binding system.

Rebinding Effect

By switching from the macroscopic to the microscopic point of view, we find out that the stochastic process modelled by (3.2) is actually **not** memoryless. That is due to the spatial arrangement of the system after a receptor-ligand-complex dissociated. Shortly after such a dissociation, it is more likely that the corresponding receptor and ligand will bind again, since they are still close to each other. Such a binding shortly after a dissociation is called a **rebinding**. The memory effect which thereby occurs is called **rebinding effect**. On large timescales, this effect diminishes since the favorable spatial situation is not given anymore and the system is more likely to be rather mixed again. Thus, Markovianity can be spoiled by the rebinding effect. It is depicted in figure 3.3.

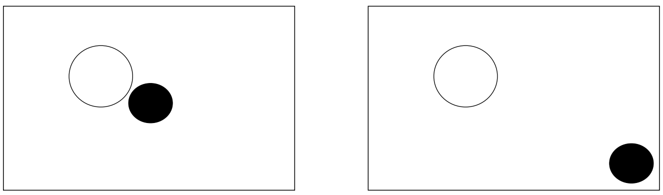

(a) Spatial constellation shortly after dissociation. (b) Spatial arrangement at an arbitrary time.

Figure 3.3: Rebinding effect: these two configurations represent the same macro state ("unbound") and are not distinguishable in model (3.2), even though different binding probabilities are expected by the receptor-ligand-distance on the microscopic scale.

This phenomenon reminds us of the recrossing effect, as described in section 1.4. As well as the recrossing effect, the rebinding effect denotes a kind of "short-time memory" caused by the spatial arrangement immediately after a transition between macro states took place. In both cases, this effect can be interpreted as the consequence of a projection: by reducing the dimension, informations about the original state space are lost and consequently, favorable spatial situations after a transition are not taken into account in the reduced model.

The rebinding effect coincides with the recrossing effect in the special context of a receptor-ligand-system. The different nomenclatures are justified by the use in their original context. While the term recrossing effect denotes the act of **recrossing** an energy barrier, the term rebinding effect denotes the **rebinding** of two molecules in a receptor-ligand-system.

In order to measure the magnitude of the rebinding effect, we interpret model (3.2) as the projection of a larger system. As demonstrated in chapter 2, a crisp clustering does not yield a correct model and should be replaced by the fuzzy approach. Accordingly, we consider the macro states “unbound” and “bound” as overlapping states. This allows a micro state to be in the “unbound” macro state with a high degree of membership to the “bound” state, for instance shortly after a dissociation, which could be interpreted as an “almost bound” state. Thus, if these states are strongly overlapping, then a high rebinding effect can be expected. In the next sections, we quantify the rebinding effect by its relation to the magnitude of overlap of the conformations.

The rebinding effect and its occurence in natural science has been described and analyzed by several authors[19, 50]. In chemistry, it has been discussed in the context of clustered receptors and clustered ligands[9, 50]. A mathematical investigation of the rebinding effect has been realized by Weber et al[55, 56].

Application: Drug Design

The term *drug design* denotes the development of new medications based on the knowledge of a biological target, playing the role of the receptor. Drug design is basically about designing a molecule which is complementary in shape and charge to the biomolecular target and therefore will bind to it[48]. More precisely, drug design describes the design of ligands, that is molecules that will bind tightly to the given target. In general, we can distinguish between the following two most common functionalities of drugs[49]:

- **Activators** are able to activate, or even deactivate, a receptor and result in a strong biological response. An example for such a drug is morphine, which acts directly to the central nervous system, mimics the actions of endorphins and thereby reduces pain.
- **Inhibitors** bind to a receptor without activating it. Though, as they “block” the binding sites of receptors, they prevent possibly disease causing particles to bind. A well-known example are protease inhibitors, a class of antiviral drugs that are widely used to treat HIV and hepatitis C.

Independently of the fact whether a drug activates or inhibits receptors, a high binding affinity is required in order to be an efficient drug. The central dogma of receptor pharmacology (“occupation theory”) is that a drug effect is directly proportional to the number of receptors that are occupied. Furthermore, a drug effect ceases as a drug-receptor complex dissociates. Thus, a low binding affinity needs to be compensated by a higher concentration of ligands, which should be avoided because of possible side effects. Accordingly, the most fundamental goal in drug design is to predict whether a given molecule will bind to a target and if so how strongly. Computational drug design[1, 7] is of particular interest, since binding interactions between molecules and receptors can be estimated on the computer, which reduces the necessity to synthesize these molecules at each step of development. One example is the newly designed nontoxic pain killer by Spahn et al[46]. In order to correctly predict binding affinities, the consideration of possible rebinding effects is essential[50, 51].

3.2 Molecular Kinetics as a Projection

In this section, we deduce a rigorous description of molecular systems, in particular receptor-ligand-systems, basically by embedding the mathematical concepts from chapter 1 into an adequate physical context. When considering such systems, we can distinguish between two points of view: we show how we can get from the *microsopic* or *atomistic* to a *macroscopic* scale by a projection. In doing so, we are particularly interested in the resulting rebinding effect included in the clustered system.

Micro States

A micro state of a molecular system with N atoms can be represented in a $6N$-dimensional *phase space* $\Gamma = \Omega \times \mathbb{R}^{3N}$, consisting of the *configuration space* $\Omega = \mathbb{R}^{3N}$ and the *momentum space* $\mathbb{R}^{3N}$. In the following, we consider systems in *thermodynamical equilibrium.* One possible model is given by the *Boltzmann distribution* $\pi : \Omega \times \mathbb{R}^{3N} \to \mathbb{R}$, a probability distribution assigning to each micro state a probability depending on its energy and temperature, see McQuarrie[28]. It can be expressed as

$$\pi(q,p) = \frac{1}{Z} \exp\left(-\beta H(q,p)\right), \tag{3.3}$$

where $\beta = 1/(k_B T)$ is the inverse of the temperature T multiplied with the Boltzmann constant k_B and $Z = \int_\Gamma \exp -\beta H(q,p)\,\mathrm{d}(q,p)$ is the normalization factor. The Hamilton function denoted by H is given by $H(q,p) = K(p) + V(q)$, the sum of the kinetic energy $K(p)$ and the potential energy $V(q)$. Thus, the Boltzmann distribution π can be decomposed into $\pi = \pi_p \pi_q$,

$$\pi(q,p) = \underbrace{\frac{1}{Z_p} \exp\left(-\beta K(p)\right)}_{\pi_p} \cdot \underbrace{\frac{1}{Z_q} \exp\left(-\beta V(q)\right)}_{\pi_q},$$

where $\pi_p : \mathbb{R}^{3N} \to \mathbb{R}$ is the probability density function of the kinetic part in the momentum space $\mathbb{R}^{3N}$ and $\pi_q : \Omega \to \mathbb{R}$ is the probability density function of the potential part in the configuration space Ω. As we are interested in examining conformations, that are objects in configuration space, we will restrict ourselves to Ω, see Huisinga[21]:

> "A conformation $C \subset \Omega$ will be identified with the particular metastable subensemble $\mu_{C\times\mathbb{R}^{3N}}$ corresponding to the particular subset $C \times \mathbb{R}^{3N} \subset \Gamma$. Hence, for every position $q \in C$, the conformation contains all states with $q \in \Omega$ and arbitrary $p \in \mathbb{R}^{3N}$."

In this sense, conformations contain no information on momenta and are determined in configuration space only. We consider a reduced model with the *reduced density* $\pi_q = \int_{\mathbb{R}^{3N}} \pi(q,p)\,\mathrm{d}p$.

Macro States via Membership Functions

As the configuration space of an average molecular system is very large, we aim to reveal the underlying discrete Markov State Model by clustering a collection of the micro states having the same or similar values in one observable. For instance, that could be the macro states "bound" or "unbound" for a simple receptor-ligand system. We apply the function-based fuzzy clustering method presented in section 2.3. We define macro states as **overlapping** partial densities, which can be identified as membership functions $\chi_1, \ldots, \chi_n : \Omega \to [0, 1]$, forming a partition of unity, i.e.

$$\sum_{i=1}^{n} \chi_i(q) = 1.$$

By grouping micro states, the corresponding macro states yield statistical weights

$$w_i = \langle \chi_i, \mathbb{1} \rangle_\pi := \int_\Omega \chi_i(q) \pi_q(q) \, \mathrm{d}q, \tag{3.4}$$

corresponding to the "probability for the system to **be** in conformation χ_i".

Transfer Operator

Each micro state $(q, p) \in \Gamma$ determines a *probability density function* $\Psi^{-\tau}(\cdot \mid (q, p))$ describing the possible evolutions of the system in configuration space Ω in time τ, being started in the initial state (q, p). Weber[53] defines a transfer operator $\mathcal{P}(\tau) : L^{1,2}_{\pi_q}(\Omega) \to L^{1,2}_{\pi_q}(\Omega)$ acting on membership functions via

$$\mathcal{P}(\tau) f(q) = \int_{\mathbb{R}^{3N}} \left(\int_\Omega f(\tilde{q}) \Psi^{-\tau}(\tilde{q} \mid (q, p)) \, \mathrm{d}\tilde{q} \right) \pi_p(p) \, \mathrm{d}p. \tag{3.5}$$

In this definition, the density function $\Psi^{-\tau}(\cdot \mid (q, p))$ can be interpreted as a transition function as defined in section 1.1. This operator corresponds to a backward transfer operator as introduced in section 1.2. It is a *generalized* transfer operator in the sense that it includes deterministic as well as stochastic dynamical models. In order to describe deterministic dynamics, the density function $\Psi^{-\tau}$ has to be chosen as a Dirac delta function, since an initial state $(q(0), p(0))$ determines exactly the future states in configuration space.

The transfer operator $\mathcal{P}(\tau)$ also defines a projected Markov operator $\overline{\mathcal{P}}(\tau)$ acting in configuration space Ω, see Weber[53], by

$$\overline{\mathcal{P}}(\tau) = \pi_q \circ \mathcal{P}(\tau) \circ (\pi_q)^{-1},$$

which propagates density functions and corresponds to a forward transfer operator. The previous equation shows that the space of membership functions is connected to the space of density functions by multiplication with π_q. We will keep that relation in mind, though just use $\mathcal{P}$ in the following.

Markov State Model for reversible Processes

Let $\mathcal{P} := \mathcal{P}(\tau)$ be the transfer operator describing a reversible process. Then $\mathcal{P}$ is self-adjoint with respect to π_q and has a real spectrum with $\sigma(\mathcal{P}) \subset [-1, 1]$, according to theorem 1.11. In order to apply the spectral approach from section 2.2, we assume that $\mathcal{P}$ has n dominant eigenvalues $1 = \lambda_1 > \lambda_2 \geq \dots \geq \lambda_n$ which are all close to 1 and bounded away from the essential spectrum. The corresponding dominant eigenfunctions are denoted by $\mathcal{X} = \{\mathcal{X}_1, \dots, \mathcal{X}_n\}$ and the eigenvalue problem is given by $\mathcal{P}\mathcal{X} = \mathcal{X}\Lambda$, with the eigenvalue matrix $\Lambda = \mathrm{diag}(\lambda_1, \dots, \lambda_n)$. As the number of metastable sets is determined by the number of dominant eigenvalues, we create a Markov State Model on n macro states. The state space of this model consists of the conformations of the molecular system and its transition behaviour is described by a $n \times n$-transition matrix $P_c := P_c(\tau)$. In order to obtain this discrete matrix from the continuous operator $\mathcal{P}$, we need at first to determine the size and shape of the membership functions χ_i. As described in section 2.3, this can be done by computing a linear combination of the dominant eigenfunctions via

$$\chi_j(q) = \sum_{i=1}^{N} A_{ij}\mathcal{X}_i(q), \ j = 1, \dots, n, \tag{3.6}$$

where the transformation matrix $A = \{A_{ij}\}_{i,j=1,\dots,n}$ is the solution of PCCA+, providing an optimal clustering. As a linear combination of orthogonal eigenfunctions $\mathcal{X}$, the membership functions χ might be overlapping; they are not orthogonal, but span the same subspace as $\mathcal{X}$. The Markov State Model is created by applying the Galerkin discretization

$$P_c = G(\mathcal{P}) = (\langle \chi, \chi \rangle_\pi)^{-1}(\langle \chi, \mathcal{P}\chi \rangle_\pi).$$

According to the proof of theorem 2.3, it can as well be written as

$$P_c = A^{-1}\Lambda A.$$

Theorem 2.3 also implies that there is no discretization error under this projection, i.e. we have $G(\mathcal{P}^k) = (P_c)^k$. In particular, Markovianity is preserved. We can use the matrix representation $P_c = S^{-1}T$ from theorem 1.17. Then S and T are stochastic matrices with

$$\begin{aligned} T &= D^{-1}\langle \chi, \mathcal{P}\chi \rangle_\pi = D^{-1}A^T\Lambda A \quad \text{and} \\ S &= D^{-1}\langle \chi, \chi \rangle_\pi = D^{-1}A^T A, \end{aligned} \tag{3.7}$$

where $D = \mathrm{diag}(w_1, \dots, w_n)$ is the diagonal matrix of statistical weights from (3.4).

Measuring the Rebinding Effect

Again, we analyze the matrix representation $P_c = S^{-1}T$ of the Markov State Model. The stochastic matrix T represents the dynamical behaviour ot the process, though the Markov State Model differs from T by

$$SP_c(\tau) = T.$$

This “deviation” of the Markov State Model $P_c(\tau)$ from the coupling matrix T is caused by the overlap of the membership functions, included in the matrix S. If S is equal to the identity matrix, then the Markov State Model is solely determined by T. If S is close to the identity matrix, then $P_c(\tau)$ is close to T and not strongly influenced by S. The more the overlap matrix S differs from the identity matrix, the more the Markov State Model $P_c(\tau)$ differs from the transition matrix T. This is due to the rebinding events. The larger this deviation, the larger the occurring memory effects. Thus, the rebinding effect, introduced in section 3.1 as a memory effect provoked by a projection, can be measured by the matrix S. The more the membership functions are overlapping, the more the matrix S deviates from the identity matrix and thereby includes stronger memory effects.

Thus, the rebinding effect can be measured by the trace of the matrix S, being the sum of its diagonal elements. It can lie between 0, implying very much rebinding, and n, implying no rebinding. This approach to measure the rebinding effect has been introduced by Weber and Fackeldey[56] and will be used in the next chapter to detect a minimal bound for the rebinding effect included in a projected system.

Infinitesimal Generator to Transition Rate Matrix

Often it is more convenient to analyze transition rate matrices instead of transition matrices. Thus, we consider the infinitesimal generator $\mathcal{Q}$, which is defined from $\mathcal{P}(\tau)$ via

$$\mathcal{Q} = \lim_{\tau \to 0} \frac{\mathcal{P}(\tau) - \mathcal{I}}{\tau}.$$

and connected by the useful relation

$$\mathcal{P}(\tau) = \exp(\tau \mathcal{Q}).$$

Since the eigenfunctions of $\mathcal{Q}$ and $\mathcal{P}$ are the same and their eigenvalues are related via $\exp(\xi_i) = \lambda_i$, we can apply the same Galerkin Projection for the infinitesimal generator as for the transfer operator. We obain a $n \times n$-matrix

$$Q_c = A^{-1} \Xi A = (\langle \chi, \chi \rangle_\pi)^{-1} (\langle \chi, \mathcal{Q} \chi \rangle_\pi), \tag{3.8}$$

where Ξ is the diagonal matrix consisting of the n leading eigenvalues $0 = \xi_1 > \xi_2 \geq \cdots \geq \xi_n$ of $\mathcal{Q}$ and A is the transformation matrix of (3.6), which analoguously transforms the eigenfunctions of $\mathcal{Q}$ into membership functions of the macro states. The clustered matrix Q_c can be interpreted as a transition rate matrix.

3.3 Minimizing the Rebinding Effect

So far, we were mainly concerned to compute the projection of a large process and, of particular interest, to analyze how such a projection introduces memory effects in the clustered process. In most of the cases though, we don't know the continuous transfer operator or infinitesimal generator describing a system. Instead, we are often given a finite matrix, for instance stemming from experimental data or, like in the example of a simple receptor-ligand system from section 3.1, as the solution of a differential equation. In either case, such a finite matrix can be **interpreted** as a projection, since it is basically a model for an originally continuous process, describing the movement of molecules in $\mathbb{R}^3$.

Assume we are in the situation that we only know the projected process Q_c. Nevertheless, we would like to know how much rebinding is included in that system, originating from the unknown projection. Since we don't know on which membership functions the projection is based on, we can only compute an estimation for that. Considering all possible membership functions, how much rebinding is included **at least** in the system?

We showed that the overlap matrix S from (3.7) provides a measure for the quantity of the rebinding effect. In particular, being close to the identity matrix implies a low rebinding, while high outer diagonal elements of S result in a high rebinding effect. In order to reveal the actual impact of the rebinding effect, we set it in relation to the stability of the clustered system Q_c. Afterwards, we formulate an optimization problem in order to deduce a lower bound for the rebinding effect included in a given system. For the sake of simplicity, we assume in the further course that the transition rates can be measured experimentally. Accordingly, we examine the given transition rate matrix Q_c of a process.

Influence of Rebinding to Stability

If the eigenvalues $\xi_i \in (-\infty, 0]$ of Q_c are close to 0, then the macro states are very stable in the sense that the probability to stay inside of such a state is close to 1. The trace of Q_c corresponds to the sum of the dominant eigenvalues of $\mathcal{Q}$. Thus, we can measure the *stability* of the molecular system by the quantity $F := -\mathrm{trace}(Q_c) \in (0, \infty)$. If F is close to 0, then the system is very stable, while it is less stable for a high value of F. We want to set the stability F in relation to the measure of the rebinding effect, the overlap matrix S.

Lemma 3.1. (Weber and Fackeldey[56])
Let Q_c be the projected infinitesimal generator of a process and $P_c(\tau)$ the corresponding projected transfer operator with the matrix representation $P_c(\tau) = S^{-1}T$, then the quantity $F := -\mathrm{trace}(Q_c)$ can be measured by

$$F = \tau^{-1}(\log(\det(S)) - \log(\det(T))), \tag{3.9}$$

if we assume that T is metastable, i.e. diagonal dominant.

Proof. We use the trace formula[2, p. 208] for matrices $\exp(\text{trace}(Q_c)) = \det(\exp(Q_c))$, the fact that Q_c "generates" $P_c(\tau)$, theorem 1.17 and multiplicativity of determinants to obtain

$$\begin{aligned}
F &= -\text{trace}(Q_c) \\
&= -\tau^{-1} \log(\exp(\text{trace}(\tau Q_c))) \\
&= -\tau^{-1} \log(\det(\exp(\tau Q_c))) \\
&= -\tau^{-1} \log(\det(P_c(\tau))) \\
&= \tau^{-1}(\log(\det(S)) - \log(\det(T))).
\end{aligned}$$

This expression is well-defined. By positive definiteness of the Gram matrix, the determinant of S lies in $(0, 1]$. The diagonal dominance of T is a natural property for a metastable process and ensures us a determinant of T in $(0, 1]$. □

Interpretation: Relevance of the Rebinding Effect

Before interpreting the result of lemma 3.1, we recall the meaning of the stochastic matrices S and T. The coupling matrix T describes the stochastic movement of the process and in particular, encodes the metastable behaviour between the conformations. Large diagonal elements result in a strong metastability and a slow process, while higher outer diagonal elements lead to faster transitions between the metastable sets. On the other hand, the overlap matrix S merely includes informations about the crispness of the membership functions, implying the magnitude of the rebinding effect.

Lemma 3.1 shows that **both** determinants of S and T influence the stability of the system, though in opposite directions. If $\det(T)$ is close to 1, then F is low and consequently the process is rather stable. If $\det(T)$ is small, then the process is rather unstable, since F is high. These relations correspond to the observations from section 2.3; a high determinant of T leads to a high metastability of the system and thus describes a slower process, while a low determinant implies higher outer diagonal elements of T and thus, makes the process faster.

In contrast, if $\det(S)$ is close to 1, then the first term in (3.9) vanishes and hence, S barely contributes to the stability, which is instead mainly determined by T. On the other hand, if $\det(S)$ is close to 0, the system becomes more stable. This means that a higher overlap of the membership functions, and thus a **strong rebinding effect**, leads to a more stable process. This relation is not obvious at first sight, yet corresponds to the qualitative description of the rebinding effect from section 3.1.

At first sight, it sounds plausible to equalize the stability of a system to its slowness. A slow system has rare transitions and thereby implies a stable system. However, a stable system does **not** necessarily imply a slow system. Instead, a rather fast system can gain a certain stability by the rebinding effect. The "fast" system has many transitions between its metastable sets. However, in case of a strong rebinding, the quitting of a metastable set can with high probability be followed by an immediate return to the previous state. Thus, the rapidness of the process can to a certain extent be compensated by the rebinding effect.

Concluding, we can differentiate between two factors leading to a high stability:

- $\det(T)$ high: The conformations have a high metastability and are well-separated. Therefore, transitions between the metastable sets are rare and the process is slow.
- $\det(S)$ low: A high rebinding effect makes the process more stable, since transitions out of a metastable set can be compensated by a fast transition back. In particular, a rapidly mixing process, $\det(T) << 1$, can be stabilized by the rebinding effect.

A stable system is naturally reached by a strongly metastable matrix T, though can likewise be obtained for a weaker metastable matrix T, if a lot of rebinding is included.

Optimization Problem: Lower Bound for the Rebinding Effect

In order to determine the stability of a system, it is of interest to know how much rebinding is included. We compute a lower bound to find out how much rebinding we are guaranteed **at least**. In order to derive an optimization problem, let us first remember how S is determined. The transfer operator $\mathcal{P}$ is projected onto a finite-dimensional state space via membership functions χ as a linear combination of the dominant eigenfunctions with a regular matrix A. Thus, the choice of the matrix A determines S and in particular the magnitude of rebinding. In order to estimate the rebinding effect included in a system, we take into consideration all *feasible* transformation matrices A, see Weber[52, chapter 3.4].

According to Weber and Fackeldey[56], we formulate an optimization problem to reveal which choice of A results in the **lowest** rebinding effect, measured by an *optimal matrix* S_{opt}. This problem is equivalent to finding the largest possible determinant of S.

Given a finite matrix Q_c, the immediate connection to the original process are the eigenvalues $\xi_1, \dots, \xi_n$, corresponding to the dominant eigenvalues of $\mathcal{Q}$. This connection is the starting point to construct the optimization problem. The eigenvalue equation of Q_c is given by

$$Q_c X = X \Xi. \tag{3.10}$$

where $\Xi = \operatorname{diag}(\xi_1, \dots, \xi_n)$. The first column of X corresponds to the first eigenvector $X_1 := (1, \dots, 1)^T$. By (3.8), we see that A^{-1} is an eigenvector matrix of Q_c as well. Therefore the columns of A^{-1} consist of multiples of the eigenvectors X_j, yielding

$$A^{-1} = \begin{pmatrix} 1 & & & \\ \vdots & \alpha_2 X_2 & \cdots & \alpha_n X_n \\ 1 & & & \end{pmatrix}$$

with $\alpha_1 = 1$ and $\alpha_2, \dots, \alpha_n \in \mathbb{R}$. We know that a determinant of S close to 1 results in a low rebinding effect. Thus, in order to find a lower bound, we try to maximize $\det(S)$, or equivalently minimize $|\det(S) - 1|$, since S is a stochastic matrix having 1 as largest possible determinant. Then the *objective function* of the optimization problem is given by

$$\boxed{\min_{\alpha_1, \dots, \alpha_n \in \mathbb{R}} |\det(S) - 1|}, \tag{3.11}$$

where several *side constraints* have to be included. As the inverse matrix A^{-1} consists of multiples of eigenvectors X_j, we have to consider

$$\boxed{\alpha_1 = 1 \quad \text{and} \quad A^{-1}_{ij} = \alpha_j X_{ij} \ \ \forall i, j}.$$

Furthermore, S is a stochastic matrix and its structure is given in terms of the linear transformation matrix A by (3.7), providing us with two further constraints

$$\boxed{S = D^{-1} A^T A \quad \text{and} \quad S_{ij} \geq 0 \ \ \forall i, j}.$$

A *feasible solution* of this optimization problem is a matrix S fullfilling all side contraints, but not necessarily being an optimum. Any feasible solution of optimization problem (3.11) will be called a *real overlap matrix* S_{real}, while an actual optimum will be called an *optimal overlap matrix* S_{opt}. Clearly, we get $\det(S_{\text{real}}) \leq \det(S_{\text{opt}}) \leq 1$.

Interpretation

The real rebinding effect is high if the determinant of S_{real} is low. Thus, a small determinant of S_{opt} implies a high rebinding effect, while a large determinant of S_{opt} gives us only few information about the actual quantity of the rebinding effect, it could be either large or small. Unfortunately, a reversible process Q_c yields a trivial solution of optimization problem (3.11) and therefore, provides us with no information, as the following theorem shows.

Theorem 3.2. **(Weber and Fackeldey[56, Theorem 1])**
Let $Q_c \in \mathbb{R}^{n \times n}$ be a reversible matrix that stems from a clustering with positive definite overlap matrix S. Then there exists a matrix $A \in \mathbb{R}^{n \times n}$ in optimization problem (3.11) *such that* $\det(S_{\text{opt}}) = 1$.

This theorem does not imply that a reversible process Q_c includes no rebinding effect. It just means that for every such process, it is possible to find a transformation matrix A yielding no rebinding. Consequently, a nontrivial estimation for the rebinding effect can be obtained only for a nonreversible system Q_c. In particular, only systems with at least three states are of interest to examine, since Q_c is reversible for $n = 2$. For instance, the example from section 3.1 describing a receptor-ligand system on two macro states “bound” and “unbound” yields the trivial solution. For that reason, we will not further examine this model, though work with a similar but slightly more complex system in the next chapter.

Using the eigenvectors of the transition rate matrix, optimization problem (3.11) is based on the assumption of an originally reversible system. In the next section, we present a generalized version based on Schur vectors. According to section 2.4, this approach includes reversible as well as non-reversible systems.

3.4 Approach for Non-reversible Processes

We extend the problem of computing the minimal rebinding effect included in a system to non-reversible processes. Employing the ideas from section 2.4, the modification of optimization problem (3.11) basically consists in a replacement of eigenvectors by Schur vectors.

Markov State Model based on Schur Decomposition

As demonstrated in the previous chapters, the fuzzy clustering method based on a spectral decomposition is not feasible for non-reversible processes. Instead, we apply the approach presented in section 2.4 to build the membership functions χ as a linear combination of real Schur vectors instead of eigenvectors.

Given a transition rate matrix $Q \in \mathbb{R}^{N\times N}$, we determine a subset $X \in \mathbb{R}^{N\times n}$ of real Schur vectors associated to the n dominant Schur values and compute the membership functions $\chi = XA$. The transformation matrix A can be obtained by Gen-PCCA, providing an optimal solution, though any other feasible matrix A yields a correct projection as well. As shown in section 2.4, a reasonable result is achieved by employing Schur vectors that are orthogonal with respect to any initial distribution η. However, considering NESS processes, we choose orthogonality with respect to the stationary distribution π.

Then, analogously to the reversible case, the projected transition rate matrix is given by

$$Q_c = \langle \chi, \chi \rangle_\pi^{-1} \langle \chi, Q\chi \rangle_\pi.$$

Since the eigenvalues of Q_c coincide with the n dominant eigenvalues of Q, it can according to the proof of theorem 2.3 as well be represented by

$$Q_c = A^{-1} \Xi_s A, \tag{3.12}$$

where Ξ_s is the Schur matrix consisting of the n dominant Schur values, i.e. eigenvalues and possibly 2×2-blocks from Q.

Minimal Rebinding Effect

Again, we are interested in the rebinding effect included in the clustered system Q_c. If we know the employed membership functions χ or the transformation matrix A, then we can easily compute the **real** rebinding effect which is encoded in the overlap matrix $S = D^{-1}A^T A$.

However, if we want to estimate the **minimal** rebinding effect included in a system Q_c, then it is not sufficient to solve optimization problem (3.11). It was based on the clustering with eigenvectors, assuming an originally reversible system, while the actual clustering is based on Schur vectors. The optimization problem has to be modified such that it is formulated in terms of Schur vectors X. We start with considering the Schur decomposition of Q_c:

$$Q_c X = X \Xi_s. \tag{3.13}$$

Comparing it to (3.12), we recognize that both X and A^{-1} are matrices of Schur vectors to the schur decomposition Ξ_s. In the last section, we exploited the analogous relation for eigenvectors to deduce that the columns of A^{-1} are multiples of the eigenvectors X. Now, having a possibly non-diagonal matrix Ξ_s, this relation does not hold anymore. We clarify this on a simple example, similar to the one from section 2.4 and containing only the dominant eigenvalue $\xi_1 = 0$ and one 2×2-block,

$$\Xi_s = \begin{pmatrix} 0 & 0 & 0 \\ 0 & \xi_2 & \epsilon \\ 0 & -\delta & \xi_3 \end{pmatrix}.$$

Given the matrix X of Schur vectors associated to Ξ_s, we aim to reveal the necessary structure of A^{-1} such that its columns are Schur vectors as well. The first Schur vector X_1, corresponding to the 1×1-block $\xi_1 = 0$, is independent of the other columns. Therefore, each multiple is a Schur vector as well. However, for our purposes the leading Schur vector should be the constant 1-vector. In contrast to that, the Schur vectors X_2 and X_3 belong to the 2×2-block and are not linear independent. Further Schur vectors for this block can be constructed as a linear combination of X_2 and X_3, according to

$$A^{-1} = \begin{pmatrix} 1 & & \\ \vdots & \alpha_2(\xi_2 X_2 - \delta X_3) & \alpha_3(\epsilon X_2 + \xi_3 X_3) \\ 1 & & \end{pmatrix}, \tag{3.14}$$

where additionally $\alpha_2 = \alpha_3$. Consequently, the computation of a column of A^{-1} depends on the corresponding Schur block. For an 1×1-block, equivalent to an eigenvalue, the column of A^{-1} is a multiple of the corresponding Schur vector. The 2×2-blocks have to be treated according to (3.14). The corresponding columns of A^{-1} are a linear combination of the two Schur vectors belonging to that block. These relations can be used to formulate the first side constraints the optimization problem needs to fulfill:
For a 1×1-block in the column j of Ξ_s, the corresponding column of A^{-1} is a multiple of the associated Schur vector X_j,

$$\boxed{\alpha_1 = 1 \quad \text{and} \quad A^{-1}_{ij} = \alpha_j X_{ij} \quad \forall i}. \tag{3.15}$$

For a 2×2-block positioned in the columns $j, j+1$ of Ξ_s, the corresponding columns of A^{-1} are built as linear combinations of the two Schur vectors X_j, X_{j+1} associated to that block:

$$\begin{gathered} \boxed{A^{-1}_{ij} = \alpha_j(\xi_j X_{ij} - \delta X_{i(j+1)}) \quad \forall i} \text{ and} \\ \boxed{A^{-1}_{i(j+1)} = \alpha_j(\epsilon X_{ij} + \xi_{j+1} X_{i(j+1)}) \quad \forall i}. \end{gathered} \tag{3.16}$$

The relation between X and A^{-1} is a bit more complicated than for a reversible process. The columns of A^{-1} are either multiples of the corresponding Schur vector for a 1×1-block or a linear combination of two Schur vectors in case of a 2×2-block. Given a Schur decomposition Ξ_s, it is necessary to detect the different blocks and compute the columns of A^{-1} accordingly.

Apart from that, the generalized optimization problem coincides with (3.11): we aim at minimizing the rebinding effect by maximizing $\det(S)$, while the side constraints guarantee the necessary structure of A, leading to a stochastic matrix S. The objective function is

$$\boxed{\min_{\alpha_1,\ldots,\alpha_n \in \mathbb{R}} |\det(S) - 1|}. \tag{3.17}$$

The entries of A^{-1} need to fulfill the side constraints (3.15) respectively (3.16), depending on the size of the corresponding Schur block. The stochastic matrix S is constructed as usual and implies the two further side constraints

$$\boxed{S = D^{-1} A^T A \quad \text{and} \quad S_{ij} \geq 0 \ \ \forall i, j}.$$

Comparison

In section 3.3, we examined originally reversible processes, clustered onto a subspace Q_c. In contrast to that, non-reversible processes are clustered in terms of Schur vectors. Then, the initial point for the optimization problem is not given by the spectral decomposition (3.10), but in terms of a Schur decomposition (3.13), with Ξ_s possibly having 2×2-blocks on its diagonal, leading to a linear dependence of the corresponding Schur vectors.

Consequently, optimization problem (3.17) requires more effort to handle, because of the necessary case distinction of different Schur blocks. However, it is a generalized version of the original formulation (3.11) and includes reversible as well as non-reversible systems. For a reversible system, they coincide. Thus, we can compute the minimal rebinding effect for **any** system, independent of the reversibility or non-reversibility of the original process.

The quality of this estimation will be evaluated in the next chapter by means of an exemplary reversible process, which will be slightly perturbed to non-reversibility by introducing such a 2×2-block. The solution of optimization problem (3.17) will be computed and compared to the outcome of the reversible case (3.11).

4 Numerical Examples

With the aim of consolidating and illustrating the results from chapter 3, we verify them on some easy examples. At first, we examine a **reversible** process and visualize some properties of the minimal rebinding effect. Afterwards, we further analyze this process, now introducing small perturbations to make it **non-reversible**, in order to observe possible consequences for the rebinding effect. As a "real-world" application, we examine a system describing the movement of **electron densities** in the chemical reaction of a molecule. Since the rebinding effect was motivated by its occurrence in ligand-binding processes, we furthermore present a **bivalent binding system** and investigate the included rebinding effect.

In the following, the minimal rebinding effect $\det(S_{\text{opt}})$ is computed as the solution of the optimization problems (3.11) and (3.17), implemented with the Matlab Optimization Toolbox.

4.1 Reversible System

Since the clustering Q_c of a reversible process Q can be non-reversible, we are interested in the relation of the rebinding effect in Q_c compared to the deviation of reversibility. This deviation will be measured by the "degree of non-reversibility" $\|DQ_c - Q_c^T D\|_1$, i.e. the deviation of detailed balance, for $D = \text{diag}(\pi_1, \ldots, \pi_n)$ being the diagonal matrix with the entries of the stationary distribution. Furthermore, we want to compare the **minimal** rebinding effect included in Q_c with the **real** rebinding effect stemming from the particular clustering, in order to evaluate the quality of this estimation.

Different clusterings of a system

Let a reversible metastable process be given by the transition matrix

$$P = \begin{pmatrix} 0.9876 & 0.0011 & 0.0011 & 0.0051 & 0.0051 \\ 0.0033 & 0.4973 & 0.4949 & 0.0036 & 0.0009 \\ 0.0033 & 0.4949 & 0.4973 & 0.0009 & 0.0036 \\ 0.0076 & 0.0018 & 0.0004 & 0.4969 & 0.4932 \\ 0.0076 & 0.0004 & 0.0018 & 0.4932 & 0.4969 \end{pmatrix}. \tag{4.1}$$

This matrix stems from Weber[54] and obviously describes a system on three metastable sets, having the dominant eigenvalues $\sigma(P) = \{1, 0.99, 0.98\}$. Accordingly, we examine different clusterings on a three-dimensional state space. For that aim, we employ several transformation matrices $A \in \mathbb{R}^{3\times 3}$, turning the dominant eigenvectors $X \in \mathbb{R}^{5\times 3}$ into membership functions $\chi \in \mathbb{R}^{5\times 3}$. In order that χ fulfills the partition of unity and non-negativity properties, the set of feasible matrices F_A has to meet certain conditions, see Weber[52, chapter 3.4]. We generate 200 random feasible transformation matrices A and examine the rebinding effect

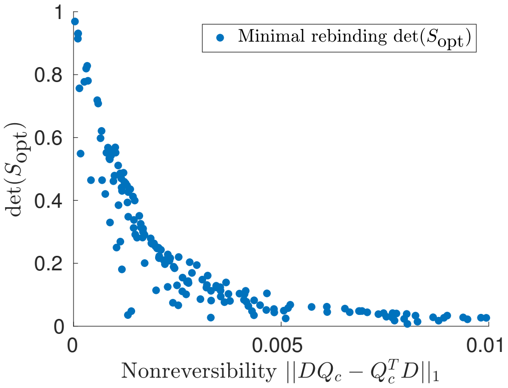

(a) The minimal rebinding effect compared to the degree of non-reversibility of the clustered system Q_c.

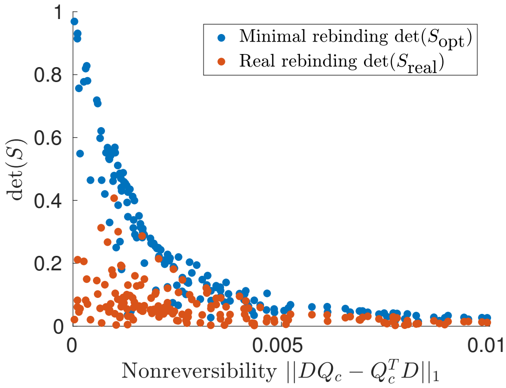

(b) The minimal and the real rebinding effect compared to the degree of non-reversibility of the clustered system Q_c.

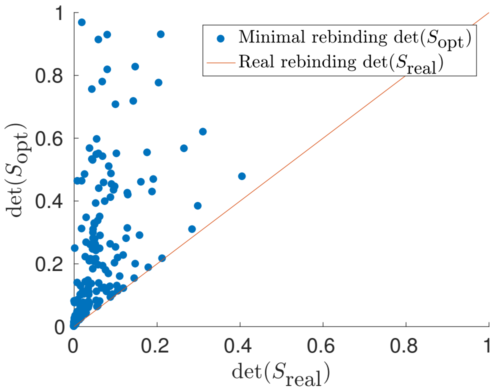

(c) The minimal rebinding effect $\det(S_{\text{opt}})$ compared to the real rebinding effect $\det(S_{\text{real}})$ included in Q_c.

Figure 4.1: The system described by the transition matrix P is clustered with 200 randomly generated feasible transformation matrices A.

caused by the projection. The results of this example are presented in figure 4.1 and can be interpreted as follows. We see in (a) that the minimal rebinding effect strongly correlates with the deviation of reversibility. The higher this degree of non-reversibility, the higher the minimal rebinding effect. This implies that for a highly non-reversible system, the minimal rebinding effect is a better estimation than for an almost reversible system, as represented in (b). However, $\det(S_{\text{opt}})$ can be a rather good or a rather bad estimation for the real rebinding effect, visible in (c).

4.2 Non-reversible System

In order to compare the rebinding effect in the clustering of a **non-reversible** system to the reversible case, we further examine the example from section 4.1. We modify it slightly by introducing small perturbations in the eigendecomposition of the reversible process, leading to non-reversibility, as proposed by Weber[54]. The outcome shall be a Schur decomposition of the shape

$$\Lambda_s = \begin{pmatrix} 1 & 0 & 0 & 0 & 0 \\ 0 & 0.99 & \epsilon & 0 & 0 \\ 0 & -\gamma & 0.98+\delta & 0 & 0 \\ 0 & 0 & 0 & 0.005 & 0 \\ 0 & 0 & 0 & 0 & 0.001 \end{pmatrix}, \tag{4.2}$$

with $\epsilon, \gamma, \delta > 0$. We compute the corresponding transition matrix by $P = X\Lambda_s X^{-1}$ with the Schur vectors X being equal to the eigenvectors from (4.1). If Λ_s is a diagonal matrix, then this equation represents the eigenvalue problem of a reversible process P. By introducing non-zero values for ϵ, γ and δ, the system gets non-reversible. This example is of particular interest, since we examine different systems, yet having the same Schur vectors and very similar Schur decompositions. However, these small changes in the Schur decomposition lead to different results when it comes to computing the rebinding effect.

Similar as in the example from section 4.1, we compute the real rebinding effect, when projecting the process onto a three-dimensional subspace represented by the transition rate matrix Q_c and compare it to the minimal rebinding effect included in that subspace. Starting from the projected process Q_c, we use the Schur vectors X from $Q_c X = X\Xi_s$, where Ξ_s is the Schur decomposition with sorted Schur values. Since Ξ_s has a 2×2 block on its diagonal, we have to solve optimization problem (3.17) based on Schur vectors to compute the minimal rebinding effect.

According to the different cases of non-reversible systems presented in section 2.4, we test the solution of this optimization problem for several parameters.

P is reversible

P is reversible if we set $\epsilon = \gamma = \delta = 0$ in the Schur decomposition (4.2). In that case, the Schur vectors are also eigenvectors of P and the system is equal to the one from the previous section. Consequently, solving the optimization problem should yield the same results when based on Schur vectors instead of eigenvectors. In order to verify that, we compute it as well for 200 clusterings with random feasible transformation matrices. The result, depicted in figure 4.2 coincides with the result from section 4.1; with an increase of non-reversibility, the minimal rebinding effect increases rather evenly, (a). The quality of that estimation can be good or bad, (c). However, the poor results are heaped around the systems Q_c which are almost reversible, (b).

Thus, if a clustered system Q_c strongly deviates from detailed balance, we can assume to obtain a rather good estimation for the rebinding effect. However, this is not at all surprising: as a lower bound, a high minimal rebinding effect $\det(S_{\text{opt}}) \approx 0$ implies a high real rebinding effect $\det(S_{\text{real}})$.

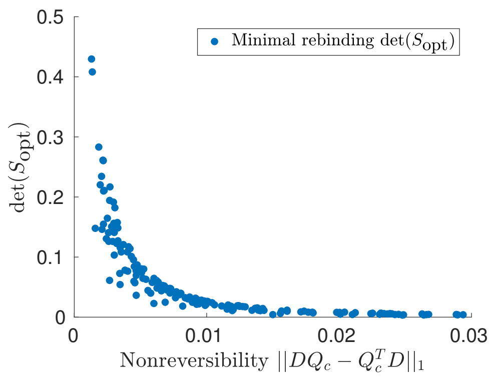

(a) The minimal rebinding effect compared to the degree of non-reversibility of the clustered system Q_c.

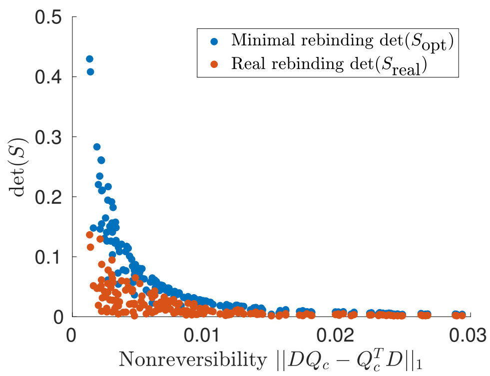

(b) The minimal and the real rebinding effect compared to the degree of non-reversibility of the clustered system Q_c.

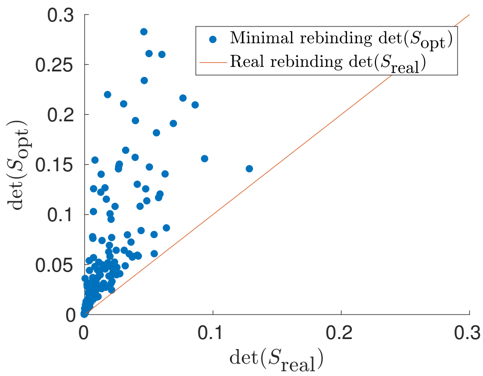

(c) The minimal rebinding effect $\det(S_{\text{opt}})$ compared to the real rebinding effect $\det(S_{\text{real}})$ included in Q_c.

Figure 4.2: The system described by the transition matrix P is clustered with 200 randomly generated feasible transformation matrices A for the values $\epsilon = 0$, $\delta = 0$.

P is nonreversible with real eigenvalues

If we set $\epsilon = 0.004$, then Λ_s is non-symmetric, leading to a non-reversible matrix P. In this case, P has still real eigenvalues, since ϵ is on the upper triangle of Λ_s.

The outcome for this system is displayed in figure 4.3. We only introduced a very small perturbation to the spectral decomposition, yet some changes in the minimal rebinding effect are clearly visible. Even though the general tendency of this estimation to change according to the degree of non-reversibility is preserved, the plot seems a bit more "fluffy". However, the general distribution of $\det(S_{\text{opt}})$ in (c) shows that again, there are good and bad estimations possible.

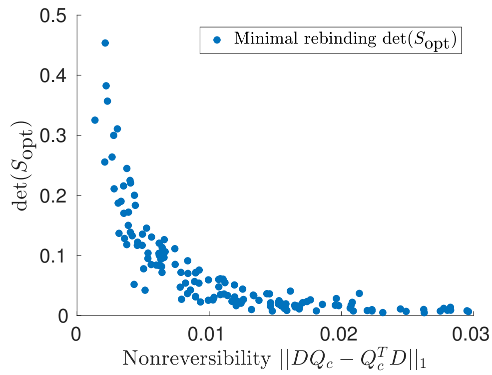

(a) The minimal rebinding effect compared to the degree of non-reversibility of the clustered system Q_c.

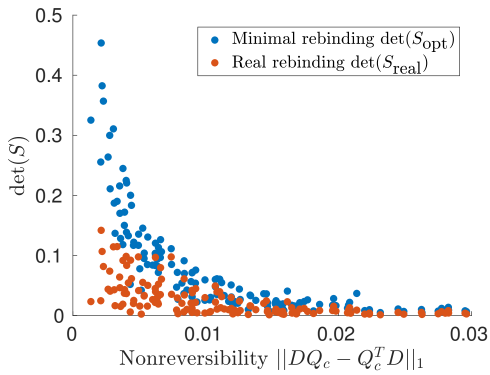

(b) The minimal and the real rebinding effect compared to the degree of non-reversibility of the clustered system Q_c.

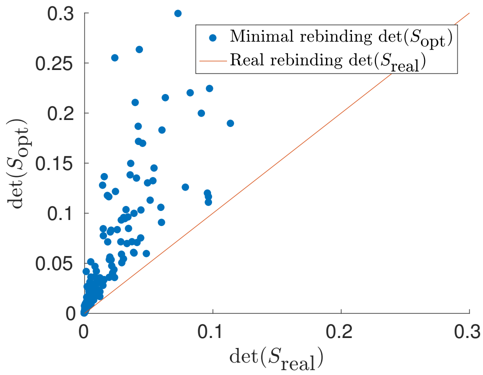

(c) The minimal rebinding effect $\det(S_{\text{opt}})$ compared to the real rebinding effect $\det(S_{\text{real}})$ included in Q_c.

Figure 4.3: The system described by the transition matrix P is clustered with 200 randomly generated feasible transformation matrices A for the values $\epsilon = 0.004$, $\delta = 0$.

P is non-diagonalizable

If we choose $\epsilon = 0.004$ and $\delta = 0.01$, then the Schur decomposition has an upper diagonal element, while the eigenvalue 0.99 occurs algebraically twice. As explained in section 2.4, this system doesn't have an eigenvalue decomposition and is not diagonalizable. Employing Schur vectors yield the result presented in figure 4.4.

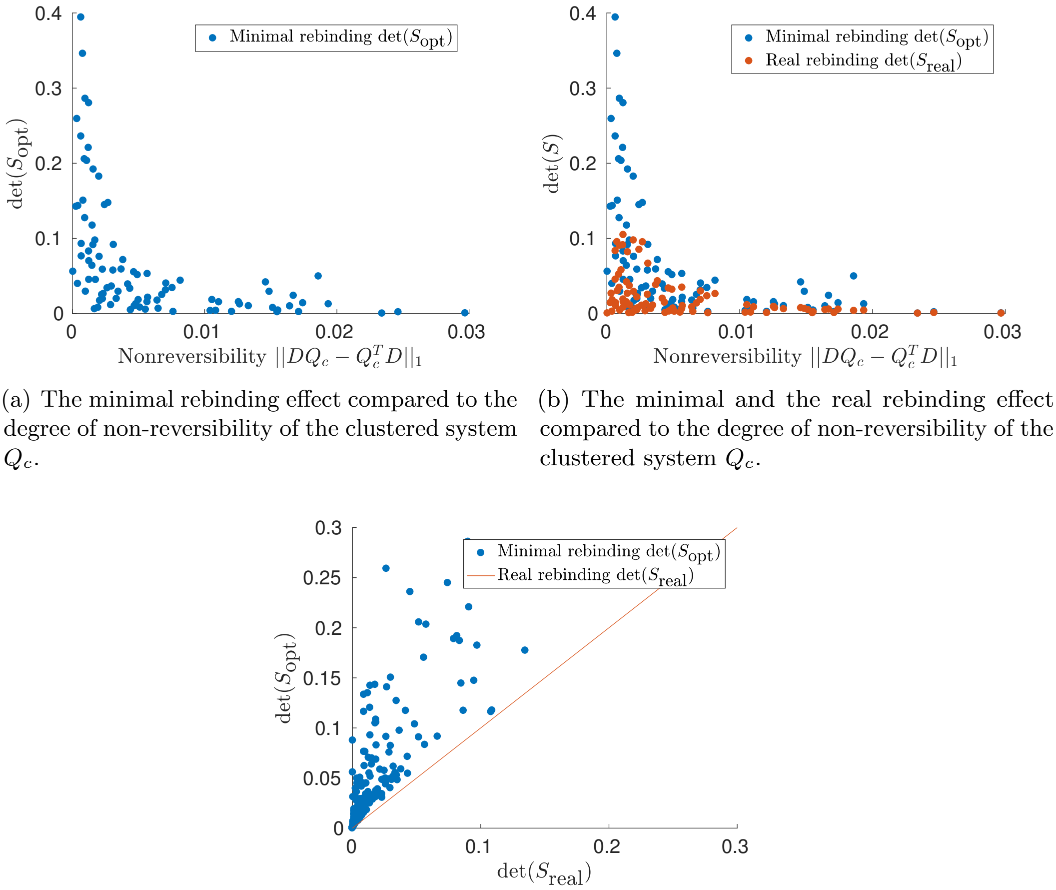

(a) The minimal rebinding effect compared to the degree of non-reversibility of the clustered system Q_c.

(b) The minimal and the real rebinding effect compared to the degree of non-reversibility of the clustered system Q_c.

(c) The minimal rebinding effect $\det(S_{\text{opt}})$ compared to the real rebinding effect $\det(S_{\text{real}})$ included in Q_c.

Figure 4.4: The system described by the transition matrix P is clustered with 200 randomly generated feasible transformation matrices A for the values $\epsilon = 0.004$, $\delta = 0.01$.

Even though the minimal rebinding effect is distributed more unevenly in (a) and (b), the estimation is not necessarily worse than before. In fact, there are some rather good estimations, visible in (c). However, the correlation between the minimal rebinding effect and the degree of nonreversibility is not as distinct as in the previous cases: while there are some good estimations for almost reversible systems, there are as well some bad estimations for rather non-reversible systems.

P is non-reversible with complex eigenvalues

Complex eigenvalues always occur in pairs and are indicated by a complete 2×2-block in the Schur decomposition. For $\epsilon = 0.004$, $\delta = 0.01$ and $\gamma = 10^{-15}$, we obtain a pair of two complex eigenvalues $0.99 + 2.3 \cdot 10^{-9}i$ and $0.99 - 2.3 \cdot 10^{-9}i$. The result, depicted in figure 4.5 shows the most "fluffy" behaviour of all examined systems. While in this case as well, the estimation can be good or bad, the correlation of the minimal rebinding effect to the degree of nonreversibility is rather weak in comparison to the preceding examples.

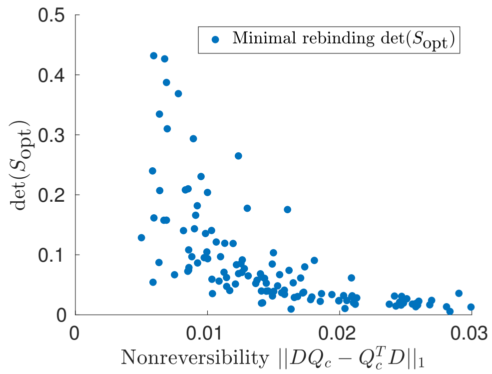

(a) The minimal rebinding effect compared to the degree of non-reversibility of the clustered system Q_c.

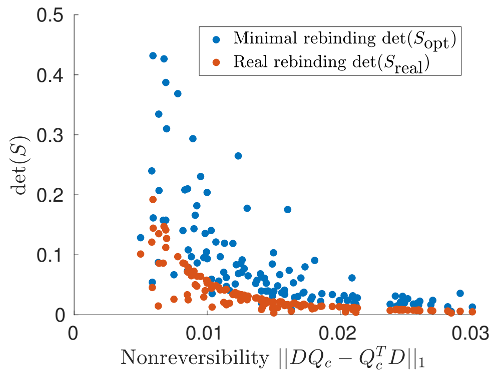

(b) The minimal and the real rebinding effect compared to the degree of non-reversibility of the clustered system Q_c.

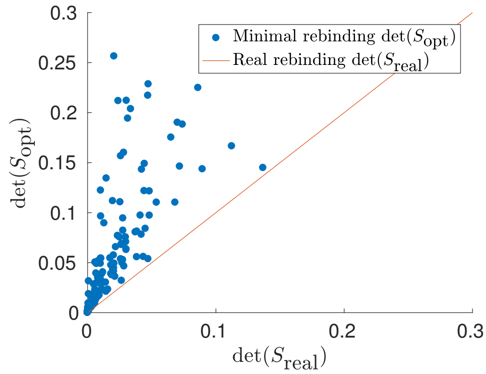

(c) The minimal rebinding effect $\det(S_{\text{opt}})$ compared to the real rebinding effect $\det(S_{\text{real}})$ included in Q_c.

Figure 4.5: The system described by the transition matrix P is clustered with 200 randomly generated feasible transformation matrices A for the values $\epsilon = 0.004$, $\delta = 0.01$ and $\gamma = 10^{-15}$.

Conclusion

The general tendency of the results is similar for all tested parameters: while the quality of the estimation can be either good or bad, there is a clearly visible correlation between the minimal rebinding effect and the non-reversibility of Q_c. However, this correlation seems to diminish the more we "perturb" the original process from reversibility. This weakened correlation implies that for originally non-reversible systems, the quality of the estimation is less predictable.

4.3 Electron Densities

The occurrence of some kind of rebinding effect can be observed in all different types of processes when projecting them. The actual meaning of this effect has to be interpreted for each system individually. We present a process describing the change of electron densities during a pericyclic chemical reaction, examined by Weber et al[57].

Formic Acid Dimer

Formic acid is a molecule consisting of one carbon atom C, two oxygen atoms O and two hydrogen atoms H. In such a system, reactions between the individual molecules take place, building hydrogen-bonded dimers, as depicted in figure 4.6. An H-atom which is attached to an O-atom moves to the O-atom of another molecule and vice versa. These reactions are caused by double proton tunneling, see Schild[37, chapter 4]. During that process, the electron density changes accordingly. This process can be represented by a reversible transition matrix

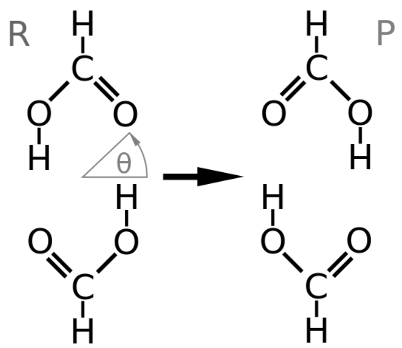

Figure 4.6: Chemical reaction in formic acid dimer. Picture taken from Weber et al[57].

P consisting of the time-dependent electron densities $\pi(t)$, as described by Weber et al[57]. Clustering it into four metastable sets using PCCA+ and transforming it into a transition rate matrix yields

$$Q_c = \begin{pmatrix} -2.0040 & 1.6859 & 0.1490 & 0.1690 \\ 1.6192 & -2.0010 & 0.1724 & 0.2095 \\ 0.1451 & 0.1747 & -1.9548 & 1.6350 \\ 0.1632 & 0.2106 & 1.6217 & -1.9955 \end{pmatrix}.$$

The membership functions of this clustering are represented depending on the angle θ in figure 4.7. We notice that the four metastable conformations correspond to the angular regions of the O-atoms. That means that high electron densities are detected around the O-atoms, which is plausible since the H-atoms tend to be attached to an O-atom.

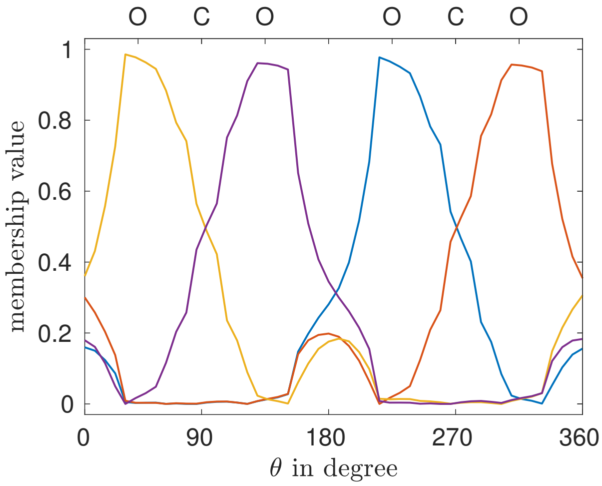

Figure 4.7: Membership functions obtained by PCCA+.

Rebinding Effect

Even though clustered with PCCA+, having the objective of maximizing the crispness, we identify rather strongly overlapping membership functions in figure 4.7 and expect a high rebinding effect. However, solving optimization problem (3.17) for Q_c yields a lower bound

$$\det(S_{\text{opt}}) = 1,$$

providing us with no information, which can be explained by the reversibility of the clustered system, $\|DQ_c - Q_c^T D\|_1 = 0$, and theorem 3.2. Knowing the membership functions χ and the stationary distribution π of the original process, we can compute the **real** rebinding effect as

$$\det(S_{\text{real}}) = D^{-1}\langle \chi, \chi \rangle_\pi = 0.2925,$$

corresponding to a strong overlap of the membership functions.

Rebinding in this context can be interpreted similar to the rebinding in receptor-ligand-systems: Shortly after a H-atom unbinds from an O-atom moving forward to the O-atom of a different molecule, it is still spatially close and attracted to its previous O-atom and therefore can rebind to it. That is one factor contributing to the stability of the four conformations. The quantitative influence of the rebinding effect on the stability of the clustered system is visualized in figure 4.8 and 4.9 for two different lag-times $\tau_1 = 0.2$ and $\tau_2 = 0.001$. The metastability of the coupling matrix T is enhanced by the significant overlap of the membership functions, yielding a strongly metastable transition matrix $P_c = S^{-1}T$. This confirms the result from section 3.1: the rebinding effect stabilizes a system by "compensating" a rather weak metastability of the conformations.

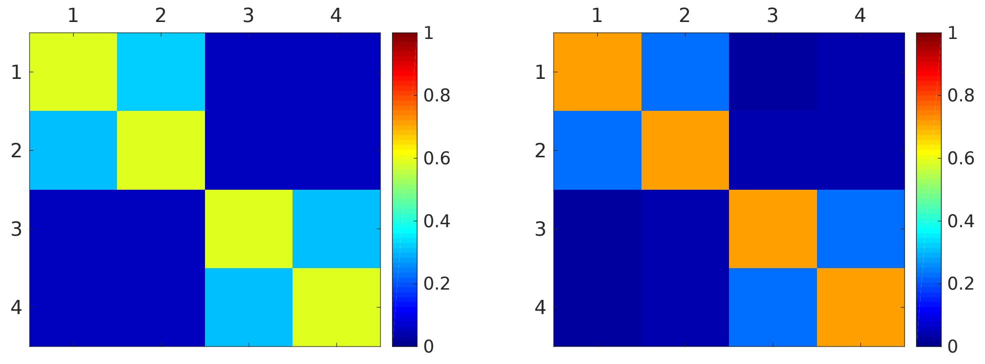

(a) Weakly metastable coupling matrix T. (b) Strongly metastable matrix $P_c = S^{-1}T$.

Figure 4.8: Coupling matrix and projected transition matrix for a lag-time $\tau_1 = 0.2$.

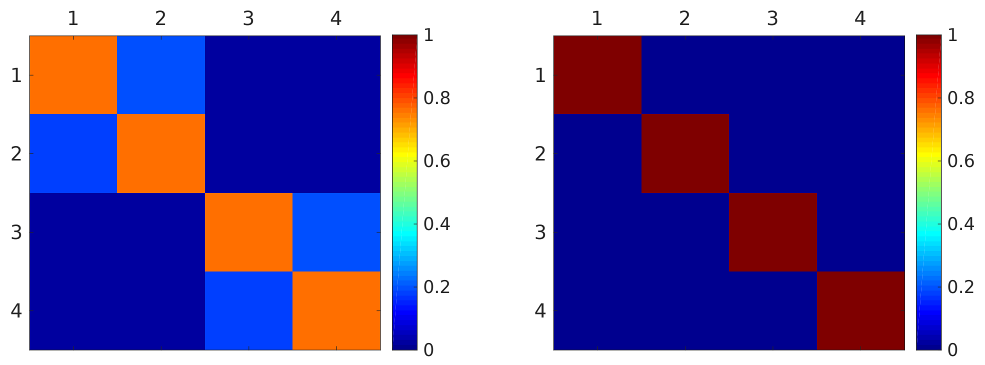

(a) Weakly metastable coupling matrix T. (b) Strongly metastable matrix $P_c = S^{-1}T$.

Figure 4.9: Coupling matrix and projected transition matrix for a small lag-time $\tau_2 = 10^{-3}$.

Metastable subset	1	2	3	4
Statistical weight	0.2406	0.2556	0.2520	0.2518
Metastability $T(\tau_1)$	0.5811	0.5827	0.5884	0.5815
Metastability $P_c(\tau_1)$	0.7077	0.7084	0.7135	0.7082
Metastability $T(\tau_2)$	0.7571	0.7577	0.7622	0.7577
Metastability $P_c(\tau_2)$	0.9980	0.9980	0.9980	0.9980

Table 4.1: Influence of rebinding to the stability of P_c for different lag-times τ_1, τ_2.

4.4 Bivalent Binding Process

Finally, we continue to examine a **ligand binding process**, being the original motivation for the investigations of the rebinding effect. In the introductional example in section 3.1, we explained the rebinding effect as a memory effect included in a system of receptors and ligands, without any structural connection of the ligands. However, the rebinding effect is conjectured to play a essential role in the context of clustered receptors and clustered ligands[9, 50].

Multivalent System

One can distinguish between **monovalent** and **multivalent** binding processes. Whenever the receptor molecules are spatially preorganized, the corresponding binding process is denoted as multivalent. A detailed summary about the key principles of multivalency can be found in Fasting et al[18].

Especially the bivalent or polyvalent case is often observed in nature. These systems are of significant interest for pharmaceutical and technical applications. If the ligands are presented multivalently as well, i.e. they are linked to each other in an appropriate way to match the preorganized receptor molecules, then often extremely high binding affinities are observed in comparison to the constituent monovalent ligands[9]. The rebinding effect is discussed to be one contributing factor for that. This is clarified in figure 4.10, representing a trivalent system.

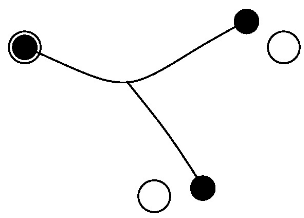

Figure 4.10: Trivalent System. From Weber and Fackeldey[56].

Imagine that the trivalent ligand is designed such that it perfectly “matches” the trivalent receptor. Shortly after one of the ligands dissociates from its receptor, it is assumed to still be spatially close to it. This effect is intensified by multivalency, since the connected ligands “keep the ligand at its place” leading to a high probability of rebinding. The rebinding effect, as explained in section 3.1 for monovalent systems, seems to be intensified by a favorable spatial preorganisation of the ligands.

The spacer connecting the ligands can be flexible or rather rigid. A rigid spacer leads to a loss of entropy of the system. The influence of multivalency to the rebinding effect was examined by Weber et al[55]. They show that using a spacer is advantageous compared to the monovalent case, though this effect is powerful especially for low affinity ligands. In that case, the rebinding effect is clearly visible, while its influence on high affinity ligands is rather limited. This result conforms with the presentation of section 3.1, establishing the impact of the rebinding effect to the stability of a system: while the rebinding effect can stabilize systems that are rather unstable, it barely contributes to stable systems.

Model of a Bivalent System

The mathematical modelling of a monovalent system is well understood, see[27, chapter 2]. Furthermore, if defined on the two macro states "unbound" and "bound", the computation of the minimal rebinding effect in such a system yields only the trivial solution, by theorem 3.2. As the the easiest multivalent case, we consider a **bivalent** process. Such a system can be described by three macro states: "unbound" (U), "singly bound" (S) and "doubly bound" (D), depicted in figure 4.11.

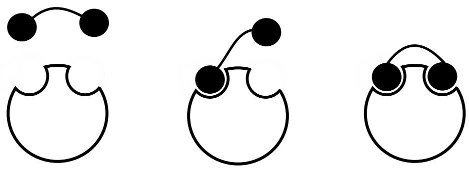

Figure 4.11: Possible macro states of a bivalent system.

This model can be represented by the reversible reactions

$$\begin{aligned} \mathrm{LL} + \mathrm{RR} &\rightleftharpoons \mathrm{L(LR)R}, \\ \mathrm{L(LR)R} &\rightleftharpoons \mathrm{(LRLR)}, \\ \mathrm{LL} + \mathrm{RR} &\rightleftharpoons \mathrm{(LRLR)}, \end{aligned} \tag{4.3}$$

with the binding rate constants k_{01} (U $\rightarrow$ S), k_{12} (S $\rightarrow$ D), k_{02} (U $\rightarrow$ D) and unbinding constants k_{10} (S $\rightarrow$ U), k_{21} (D $\rightarrow$ S), k_{20} (D $\rightarrow$ U), resulting in a transition rate matrix

$$Q_c = \begin{pmatrix} -(k_{01}+k_{02})[\mathrm{RR}] & k_{01}[\mathrm{RR}] & k_{02}[\mathrm{RR}] \\ k_{10} & -(k_{10}+k_{12}) & k_{12} \\ k_{20} & k_{21} & -(k_{20}+k_{21}) \end{pmatrix},$$

depending on the concentrations of the bivalent receptor molecules [RR]. This matrix is constructed in the same fashion as explained in section 3.1 for the monovalent case and likewise describes changes of concentrations by the ordinary differential equation

$$\dot{x}^T = x^T Q_c.$$

The vector $x^T = ([\mathrm{LL}], [\mathrm{L(LR)R}], [\mathrm{(LRLR)}])$ consists of the initial concentrations of unbound ligands [LL], singly bound ligands [L(LR)R] and doubly bound ligands [(LRLR)]. For realistic applications, we assume to start with a system where only unbound ligands are inserted and the changes of concentrations are observed.

Considering Q_c, we are in the situation that we are given a process which can be **interpreted** as a projection, while we do not know the original process and therefore cannot compute the actual rebinding effect. However, we presume that by the unknown projection, there is some rebinding effect included in Q_c. Assuming a clustering in terms of overlapping membership functions $\chi = XA$, we again solve optimization problem (3.17) to obtain the minimal rebinding effect as an estimation.

Artificial Bivalent Binding Process

Model (4.3) is tested with different binding and unbinding constants shown in table 4.2. They represent systems with rather strong association and low dissociation behaviour. For all three systems, we employ the same binding constants and only slightly modify the dissociation constants. In figure 4.12, we can see that all three systems show a rather similar behaviour; the minimal rebinding effect decreases with increased receptor concentrations. However, even though the differences between the systems are not large, $\det(S_{\text{opt}})$ differs quite strongly.

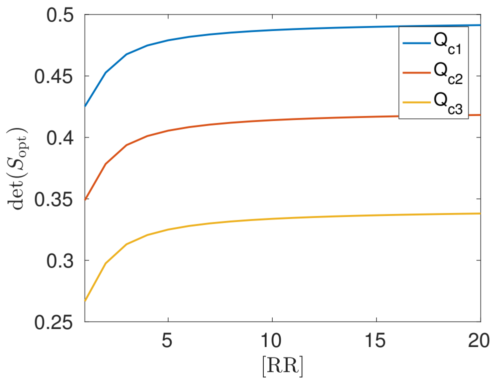

Figure 4.12: The minimal rebinding effect of different systems Q_c depending on the concentration [RR] of receptor molecules.

Binding constant	k_{01}	k_{10}	k_{12}	k_{21}	k_{02}	k_{20}
Q_{c_1}	0.08	0.006	0.09	0.011	0.01	0.001
Q_{c_2}	0.08	0.005	0.09	0.010	0.01	0.001
Q_{c_3}	0.08	0.004	0.09	0.009	0.01	0.001

Table 4.2: Different binding constants between the three macro states “unbound”, “singly bound” and “doubly bound”.

With an increasing concentration of receptor molecules, the minimal rebinding effect decreases. That seems plausible: in a system with a large concentration of receptors, a ligand dissociating from a receptor is more likely to be immediately close to a different receptor and bind to it instead of rebind. Even though this result sounds persuasive, it does not take into account the nature of model (4.3). From a mathematical point of view, binding events between different receptors are **indistinguishable** under this model. In simple terms, this model “does not know” if a binding is a rebinding or a binding to a different receptor. Instead, according to Weber and Fackeldey[56], the decreasing rebinding effect presented in figure 4.12 can be explained by a decrease in the transition regions between the binding events caused by the increased receptor concentration.

For **low** receptor concentrations the result is reasonable though: in that case, bindings shortly after a dissociation are likely to be a rebinding, since there are no other receptors nearby. However, that is a rather theoretical consideration, since in realistic models we expect a higher concentration of receptors.

Real Bivalent Binding Process

One example representing a bivalent-receptor bivalent-ligand system is shown in figure 4.4. This presentation also demonstrates the flexibility of the spacer. For more informations about the benefits of using of a spacer, see Weber et al[55] or Bujotzek[8]. In order to examine the

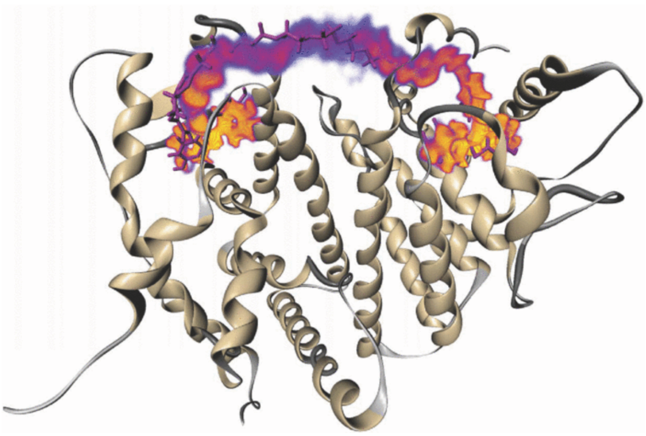

Figure 4.13: Estrogen receptor in complex with a bivalent raloxifene ligand. The spacer is represented by the configuration density cloud (orange: rigid parts, purple: flexible parts). The picture is taken from Weber et al[55].

rebinding effect included in this receptor-ligand system, we need to obtain the binding and unbinding constants for model (4.3). This can be achieved by simulations or experiments. For the resulting transition rate matrix Q_c, the minimal rebinding effect can be computed. However, we have to face the following problems: from the previous sections, we know that the minimal rebinding effect $\det(S_{\text{opt}})$ can be a good or a bad estimation and hence, we cannot rely on it. Furthermore, the computed rebinding effect does not provide the desired informations for large receptor concentrations. Consequently, instead of continuing to use this model, we should aim to create a new model including the relevant spatial informations.

Interpretation

The kind of rebinding effect that we are interested in includes spatial informations. A rebinding in that sense means that a ligand is still **spatially close** to the receptor from which it unbound. In contrast to that, the presented model (4.3) for a bivalent binding process includes no spatial informations; consequently, the kind of rebinding effect included in that system is different from the one we introduced in section 3.1. It is like an additional memory between the observables “unbound” and “bound”, without being able to distinguish between bindings to different receptors.

Accordingly, we have to differentiate between different kinds of rebinding: The rebinding effect, as introduced in section 3.1 can be interpreted as a “spatial memory” and this is the kind of rebinding we are interested in. In the general case though, the interpretation of the rebinding effect for a system depends on the choice of the macro states: it can be interpreted as a “memory between the macro states”. For this reason, we have to carefully choose the macro states on which we are creating a model. If we want to include the rebinding effect as a spatial memory, the macro states should represent spatial informations as well.

For instance, in the previous example describing a chemical reaction, we observed four conformations corresponding to the four **spatially** arranged O-atoms. Rebinding in this model means that electrons unbinding from an O-atom return to it with a certain probability instead of binding to the next one. Therefore, the rebinding effect in this context corresponds to the characterization from section 3.1.

There are different approaches which could be followed in order to correctly describe the rebinding effect in a receptor-ligand system. The construction of a more extensive model on macro states including spatial informations could be a reasonable solution, though it is not straight-forward to create such a model. Another option would be to switch from the molecular kinetics to the molecular dynamics approach in order to obtain more informations about the rebinding effect by simulations.

Conclusion

In this thesis, two recent research topics were combined by extending the computation of a lower bound for the rebinding effect onto non-reversible processes. The procedure of projecting a process onto its metastable sets in terms of membership functions has been elaborately described. In doing so, the generalized fuzzy clustering algorithm GenPCCA has been employed, yielding the optimal membership functions as a linear combination of the dominant Schur vectors and including non-reversible processes. The overlap of the membership functions is crucial for a correct mapping, though influences the observed stability of the system. The more overlap, the more stable the macro states appear to be.

This phenomenon is denoted as **rebinding effect** because of its occurrence in receptor-ligand-systems, where this "spatial memory" leads to an increased probability for a fast rebinding after the dissociation of a receptor-ligand-complex. Under the assumption of a fuzzy clustering $\chi = XA$, the minimal rebinding effect included in a given kinetics has been computed as the solution of an optimization problem, considering reversible as well as non-reversible processes by using Schur vectors X. This optimization problem has been implemented and tested for some illustrative examples, demonstrating the prospects and indicating the limitations of this method.

Knowing the rebinding effect of a system can be of particular relevance for applications like computational drug design, where it is important to correctly predict binding affinities in order to evaluate the expected efficiency of a newly designed drug. Since many real-world processes are non-reversible, it was important to add this case to the already existing optimization problem for reversible processes. This extension yields an estimation for the rebinding effect of a clustered system, without the necessity to know if the original process was actually reversible or non-reversible.

With the existing molecular kinetics models for receptor-ligand-systems, it is not readily possible to determine the rebinding effect in the desired way. Even though the rebinding effect is mathematically well understood, it is still difficult to include it adequately into real binding processes, which is due to the modelling problems. When creating such a model, the macro states should contain spatial informations. Additionally to the issue of finding a suitable model, we still have to face the problem that the minimal rebinding effect is not always a good estimation for the real rebinding effect.

While the focus of this thesis lies on the molecular kinetics point of view, it seems promising to combine it with the molecular dynamics approach in order to further advance the study of the rebinding effect. Especially for rather complex multivalent systems, being of high interest for drug design, a simulation-based method could be useful.

Bibliography

[1] K. Andrae, V. Durmaz, K. Fackeldey, O. Scharkoi, and M. Weber, *Medizin aus dem computer*, Der Schmerz, 27 (2013), pp. 409–413.

[2] G. B. Arfken, H. J. Weber, and F. E. Harris, *Mathematical methods for physicists*, Academic Press, 1995.

[3] R. E. Bellman, *Adaptive control processes: a guided tour*, Princeton university press, 2015.

[4] V. I. Bogachev, *Measure theory*, vol. 1, Springer Science & Business Media, 2007.

[5] G. R. Bowman, V. S. Pande, and F. Noé, *An introduction to Markov state models and their application to long timescale molecular simulation*, vol. 797, Springer Science & Business Media, 2013.

[6] J. H. Brandts, *Matlab code for sorting real schur forms*, Numerical linear algebra with applications, 9 (2002), pp. 249–261.

[7] N. Brown, *In Silico Medicinal Chemistry: Computational Methods to Support Drug Design*, no. 8 in Theoretical and Computational Chemistry Series, Royal Society of Chemistry, 2015.

[8] A. Bujotzek, *Molecular Simulation of Multivalent Ligand-Receptor Systems*, PhD thesis, Freie Universität Berlin, 2013.

[9] B. R. Caré and H. A. Soula, *Impact of receptor clustering on ligand binding*, BMC Systems Biology, 5 (2011), p. 48.

[10] J. D. Chodera and F. Noé, *Markov state models of biomolecular conformational dynamics*, Current opinion in structural biology, 25 (2014), pp. 135–144.

[11] L.-T. Da, F. K. Sheong, D.-A. Silva, and X. Huang, *Application of markov state models to simulate long timescale dynamics of biological macromolecules*, in Protein Conformational Dynamics, Springer, 2014, pp. 29–66.

[12] M. Dellnitz and O. Junge, *On the approximation of complicated dynamical behavior*, SIAM Journal on Numerical Analysis, 36 (1999), pp. 491–515.

[13] P. Deuflhard, W. Huisinga, A. Fischer, and C. Schütte, *Identification of almost invariant aggregates in reversible nearly uncoupled markov chains*, Linear Algebra and its Applications, 315 (2000), pp. 39–59.

[14] P. Deuflhard and M. Weber, *Robust perron cluster analysis in conformation dynamics*, Linear algebra and its applications, 398 (2005), pp. 161–184.

[15] N. Djurdjevac Conrad, M. Weber, and C. Schütte, *Finding dominant structures of nonreversible markov processes*, Multiscale Modeling & Simulation, 14 (2016), pp. 1319–1340.

[16] K. Fackeldey and M. Weber, *GenPCCA – markov state models for non-equilibrium steady states*, WIAS Report, 29 (2017), pp. 70–80.

[17] K. Fackeldey and M. Weber, *Molecular kinetics for non-reversible chemical processes*, Submitted for publication, (2017).

[18] C. Fasting, C. A. Schalley, M. Weber, O. Seitz, S. Hecht, B. Koksch, J. Dernedde, C. Graf, E.-W. Knapp, and R. Haag, *Multivalency as a chemical organization and action principle*, Angewandte Chemie International Edition, 51 (2012), pp. 10472–10498.

[19] B. Goldstein and M. Dembo, *Approximating the effects of diffusion on reversible reactions at the cell surface: ligand-receptor kinetics.*, Biophysical Journal, 68 (1995), p. 1222.

[20] G. H. Golub and C. F. van Loan, *Matrix Computations*, The John Hopkins University Press, Baltimore and London, 1996.

[21] W. Huisinga, *Metastability of markovian systems*, Ph.D. thesis, Freie Universität Berlin, (2001).

[22] W. Huisinga and B. Schmidt, *Metastability and dominant eigenvalues of transfer operators*, in New Algorithms for Macromolecular Simulation, Springer, 2006, pp. 167–182.

[23] S. L. Kalpazidou, *Cycle representations of Markov processes*, vol. 28, Springer Science & Business Media, 2007.

[24] T. Kato, *Perturbation Theory for Linear Operators*, Classics in Mathematics. Springer, 1995.

[25] F. P. Kelly, *Reversibility and Stochastic Networks*, Wiley, 1979.

[26] O. Knill, *Probability and stochastic processes with applications*, Havard Web-Based, (1994).

[27] D. A. Lauffenburger and J. Linderman, *Receptors: models for binding, trafficking, and signaling*, Oxford University Press, 1993.

[28] D. A. McQuarrie, *Statistical Mechanics*, University Science Books, California, 2000.

[29] S. P. Meyn and R. L. Tweedie, *Markov Chains and Stochastic Stability*, Communications and Control Engineering Series. Springer, 1993.

[30] A. Nielsen, *Computation schemes for transfer operators*, Ph.D. thesis, Freie Universität Berlin, (2015).

[31] B. Øksendal, *Stochastic differential equations*, Springer, 2003.

[32] J.-H. Prinz, H. Wu, M. Sarich, B. Keller, M. Senne, M. Held, J. D. Chodera, C. Schütte, and F. Noé, *Markov models of molecular kinetics: Generation and validation*, The Journal of chemical physics, 134 (2011), p. 174105.

[33] S. Röblitz, *Statistical error estimation and grid-free hierarchical refinement in conformation dynamics*, PhD thesis, Freie Universität Berlin, 2009.

[34] S. Röblitz and M. Weber, *Fuzzy spectral clustering by PCCA+: application to markov state models and data classification*, Advances in Data Analysis and Classification, 7 (2013), pp. 147–179.

[35] M. Sarich, *Projected transfer operators*, PhD thesis, Freie Universität Berlin, 2011.

[36] M. Sarich, R. Banisch, C. Hartmann, and C. Schütte, *Markov state models for rare events in molecular dynamics*, Entropy, 16 (2013), pp. 258–286.

[37] A. Schild, *Electron fluxes during chemical processes in the electronic ground state*, Ph.D. thesis, Freie Universität Berlin, (2013).

[38] I. Schur, *On the characteristic roots of a linear substitution with an application to the theory of integral equations*, Math. Ann, 66 (1909), pp. 488–510.

[39] C. Schütte, *Conformational dynamics: Modelling, theory, algorithm, and application to biomolecules*, Habilitation thesis, Freie Universität Berlin, (1998).

[40] C. Schütte, A. Fischer, W. Huisinga, and P. Deuflhard, *A direct approach to conformational dynamics based on hybrid monte carlo*, Journal of Computational Physics, 151 (1999), pp. 146–168.

[41] C. Schütte, W. Huisinga, and P. Deuflhard, *Transfer operator approach to conformational dynamics in biomolecular systems*, in Ergodic theory, analysis, and efficient simulation of dynamical systems, Springer, 2001, pp. 191–223.

[42] C. Schütte and M. Sarich, *Metastability and Markov State Models in Molecular Dynamics: Modeling, Analysis, Algorithmic Approaches*, vol. 24 of Courant Lecture Notes, American Mathematical Soc., 2013.

[43] M. Shan, A. Bujotzek, F. Abendroth, A. Wellner, R. Gust, O. Seitz, M. Weber, and R. Haag, *Conformational analysis of bivalent estrogen receptor ligands: from intramolecular to intermolecular binding*, ChemBioChem, 12 (2011), pp. 2587–2598.

[44] D. E. Shaw, R. O. Dror, J. K. Salmon, J. Grossman, K. M. Mackenzie, J. A. Bank, C. Young, M. M. Deneroff, B. Batson, K. J. Bowers, et al.,

Millisecond-scale molecular dynamics simulations on anton, in High performance computing networking, storage and analysis, proceedings of the conference on, IEEE, 2009, pp. 1–11.

[45] D. E. Shaw, J. Grossman, J. A. Bank, B. Batson, J. A. Butts, J. C. Chao, M. M. Deneroff, R. O. Dror, A. Even, C. H. Fenton, et al., *Anton 2: raising the bar for performance and programmability in a special-purpose molecular dynamics supercomputer*, in Proceedings of the international conference for high performance computing, networking, storage and analysis, IEEE Press, 2014, pp. 41–53.

[46] V. Spahn, G. Del Vecchio, D. Labuz, A. Rodriguez-Gaztelumendi, N. Massaly, J. Temp, V. Durmaz, P. Sabri, M. Reidelbach, H. Machelska, et al., *A nontoxic pain killer designed by modeling of pathological receptor conformations*, Science, 355 (2017), pp. 966–969.

[47] G. W. Stewart and J.-G. Sun, *Matrix Perturbation Theory*, Computer Science and Scientific Computing. Academic Press Boston, 1990.

[48] K. Strømgaard, P. Krogsgaard-Larsen, and U. Madsen, *Textbook of Drug Design and Discovery*, CRC Press, 2002.

[49] J. Tollenaere, *The role of structure-based ligand design and molecular modelling in drug discovery*, Pharmacy World and Science, 18 (1996), pp. 56–62.

[50] G. Vauquelin, *Rebinding: or why drugs may act longer in vivo than expected from their in vitro target residence time*, Expert Opinion on Drug Discovery, 5 (2010), pp. 927–941.

[51] G. Vauquelin and S. J. Charlton, *Long-lasting target binding and rebinding as mechanisms to prolong in vivo drug action*, British journal of pharmacology, 161 (2010), pp. 488–508.

[52] M. Weber, *Meshless methods in conformation dynamics*, Ph.D. thesis, Freie Universität Berlin, (2006).

[53] M. Weber, *A subspace approach to molecular markov state models via a new infinitesimal generator*, Habilitation thesis, Freie Universität Berlin, (2011).

[54] M. Weber, *Eigenvalues of non-reversible markov chains – a case study*, Tech. Report 17-13, ZIB, 2017.

[55] M. Weber, A. Bujotzek, and R. Haag, *Quantifying the rebinding effect in multivalent chemical ligand-receptor systems*, The Journal of Chemical Physics, 137 (2012).

[56] M. Weber and K. Fackeldey, *Computing the minimal rebinding effect included in a given kinetics*, Multiscale Modeling & Simulation, 12 (2014), pp. 318–334.

[57] M. Weber, A. Schild, H. Rust, and K. Fackeldey, *From metastable to coherent sets - time-discretization schemes*, In preparation, (2017).

[58] D. Werner, *Funktionalanalysis*, Springer, 2006.

Selbstständigkeitserklärung

Hiermit bestätige ich, dass ich die vorliegende Arbeit selbstständig verfasst habe und keine anderen als die angegebenen Quellen und Hilfsmittel benutzt habe. Die Arbeit wurde bisher in gleicher oder ähnlicher Form keiner anderen Prüfungskommission vorgelegt und auch nicht veröffentlicht.

Berlin, den 4. September 2017

Susanne Röhl